2014

Interferon regulatory factor 5-dependent immune responses in the draining lymph node protect against West Nile Virus infection

Larissa B. Thackray
Washington University School of Medicine in St. Louis

Bimmi Shrestha
Washington University School of Medicine in St. Louis

Justin M. Richner
Washington University School of Medicine in St. Louis

Jonathan J. Miner
Washington University School of Medicine in St. Louis

Amelia K. Pinto
Washington University School of Medicine in St. Louis

See next page for additional authors

Authors
Larissa B. Thackray, Bimmi Shrestha, Justin M. Richner, Jonathan J. Miner, Amelia K. Pinto, Helen M. Lazear, and Michael Gale Jr.

Journal of Virology

Interferon Regulatory Factor 5-Dependent Immune Responses in the Draining Lymph Node Protect against West Nile Virus Infection

Larissa B. Thackray, Bimmi Shrestha, Justin M. Richner, Jonathan J. Miner, Amelia K. Pinto, Helen M. Lazear, Michael Gale Jr. and Michael S. Diamond

J. Virol. **2014, 88(19):11007. DOI: 10.1128/JVI.01545-14. Published Ahead of Print 16 July 2014.**

JVI Journals.ASM.org

Interferon Regulatory Factor 5-Dependent Immune Responses in the Draining Lymph Node Protect against West Nile Virus Infection

Larissa B. Thackray,[a] Bimmi Shrestha,[a] Justin M. Richner,[a] Jonathan J. Miner,[a] Amelia K. Pinto,[a] Helen M. Lazear,[a] Michael Gale, Jr.,[e] Michael S. Diamond[a,b,c,d]

Departments of Medicine,[a] Molecular Microbiology,[b] Pathology and Immunology,[c] and The Center for Human Immunology and Immunotherapy Programs,[d] Washington University School of Medicine, Saint Louis, Missouri, USA; Department of Immunology, University of Washington School of Medicine, Seattle, Washington, USA[e]

ABSTRACT

Upon activation of Toll-like and RIG-I-like receptor signaling pathways, the transcription factor IRF5 translocates to the nucleus and induces antiviral immune programs. The recent discovery of a homozygous mutation in the immunoregulatory gene guanine exchange factor dedicator of cytokinesis 2 (*Dock2*$^{mu/mu}$) in several *Irf5*$^{-/-}$ mouse colonies has complicated interpretation of immune functions previously ascribed to IRF5. To define the antiviral functions of IRF5 *in vivo*, we infected backcrossed *Irf5*$^{-/-}$ × *Dock2*$^{wt/wt}$ mice (here called *Irf5*$^{-/-}$ mice) and independently generated CMV-Cre *Irf5*$^{fl/fl}$ mice with West Nile virus (WNV), a pathogenic neurotropic flavivirus. Compared to congenic wild-type animals, *Irf5*$^{-/-}$ and CMV-Cre *Irf5*$^{fl/fl}$ mice were more vulnerable to WNV infection, and this phenotype was associated with increased infection in peripheral organs, which resulted in higher virus titers in the central nervous system. The loss of IRF5, however, was associated with only small differences in the type I interferon response systemically and in the draining lymph node during WNV infection. Instead, lower levels of several other proinflammatory cytokines and chemokines, as well as fewer and less activated immune cells, were detected in the draining lymph node 2 days after WNV infection. WNV-specific antibody responses in *Irf5*$^{-/-}$ mice also were blunted in the context of live or inactivated virus infection and this was associated with fewer antigen-specific memory B cells and long-lived plasma cells. Our results with *Irf5*$^{-/-}$ mice establish a key role for IRF5 in shaping the early innate immune response in the draining lymph node, which impacts the spread of virus infection, optimal B cell immunity, and disease pathogenesis.

IMPORTANCE

Although the roles of IRF3 and IRF7 in orchestrating innate and adaptive immunity after viral infection are established, the function of the related transcription factor IRF5 remains less certain. Prior studies in *Irf5*$^{-/-}$ mice reported conflicting results as to the contribution of IRF5 in regulating type I interferon and adaptive immune responses. The lack of clarity may stem from a recently discovered homozygous loss-of-function mutation of the immunoregulatory gene *Dock2* in several colonies of *Irf5*$^{-/-}$ mice. Here, using a mouse model with a deficiency in IRF5 and wild-type Dock2 alleles, we investigated how IRF5 modulates West Nile virus (WNV) pathogenesis and host immune responses. Our *in vivo* studies indicate that IRF5 has a key role in shaping the early proinflammatory cytokine response in the draining lymph node, which impacts immunity and control of WNV infection.

A canonical model for type I IFN production after virus infection is a two-step positive feedback loop that is regulated by Interferon regulatory factor 3 (IRF3) and IRF7 (1). Detection of viral nucleic acids by Toll-like receptors (TLRs), RIG-I-like (RLRs) receptors, or DNA sensors induces nuclear localization of IRF3, which in concert with NF-κB and ATF-2/c-Jun stimulates transcription, synthesis, and secretion of IFN-β by infected cells. Extracellular interferon beta (IFN-β) binds to the type I IFN receptor (IFNAR) and triggers activation of the JAK-STAT signaling pathway and induction of IFN-stimulated genes (ISGs) (2), which inhibit viral entry, translation, replication, and assembly through a variety of independent mechanisms (reviewed in reference 3). While IRF3 is constitutively expressed in many tissues, IRF7 is an ISG required for the expression of most IFN-α subtypes and is thus a key mediator of the type I IFN amplification loop (1, 4).

Noncanonical signaling pathways also induce type I IFN responses. Even with genetic ablation of IRF3 and IRF7 (*Irf3*$^{-/-}$ × *Irf7*$^{-/-}$ double-knockout [DKO] cells or mice), type I IFN was produced after infection with West Nile virus (WNV), dengue virus, murine norovirus, or murine cytomegalovirus, albeit at reduced levels compared to wild-type (WT) cells and mice (5–8). Consistent with the sustained production of type I IFN, lethality in *Irf3*$^{-/-}$ × *Irf7*$^{-/-}$ DKO mice infected with WNV or Chikungunya virus was not as rapid or complete as in *Ifnar*$^{-/-}$ mice (5, 9–11). *Ex vivo* experiments with primary myeloid dendritic cells and macrophages revealed that the IFN-β response after WNV infection was maintained in DKO cells but abrogated in the absence of MAVS (5, 12). The transcription factors ELF4 and IRF5 both have been implicated as participants in the MAVS-dependent induction of IFN-β after WNV infection. A deficiency of ELF4 resulted in reduced type I IFN production after WNV infection in mice (13). ELF4 translocates into the nucleus after MAVS-dependent activation, binds to IFN promoters, and cooperatively increases

Received 28 May 2014 Accepted 13 July 2014
Published ahead of print 16 July 2014
Editor: R. W. Doms
Address correspondence to Michael S. Diamond, diamond@borcim.wustl.edu.

doi:10.1128/JVI.01545-14

the binding affinity of IRF3 and IRF7 (13). Mice or cells lacking IRF3, IRF5, and IRF7 ($Irf3^{-/-} \times Irf5^{-/-} \times Irf7^{-/-}$ triple-knockout [TKO] cells or mice) had abrogated type I IFN and ISG expression in dendritic cells and serum after WNV infection, although an IFN response still persisted in macrophages (14).

Activation of IRF5 in myeloid cells also induces proinflammatory cytokine expression downstream of TLR7 and MyD88 signaling through a TRAF6- and IRAK1-dependent mechanism (15–19). In an original study of immune cells from $Irf5^{-/-}$ mice, IFN-α levels were normal after TLR stimulation although interleukin-6 (IL-6), IL-12, and tumor necrosis factor alpha (TNF-α) levels were reduced (18). Subsequent experiments suggested that IRF5 regulates type I IFN production *in vivo* after viral infection (20, 21), and a lack of this function in $Irf5^{-/-}$ mice was associated with enhanced susceptibility to infection with vesicular stomatitis virus (VSV) or herpes simplex virus (HSV). In response to Newcastle disease virus (NDV) infection, IRF5 induced overlapping and distinct sets of genes compared to IRF7, including the induction of type I IFN and proinflammatory cytokines (20, 22).

Two recent studies revealed the emergence of a spontaneous genomic duplication and frameshift mutation in the guanine exchange factor dedicator of cytokinesis 2 (*Dock2*) that arose in at least a subset of $Irf5^{-/-}$ mouse colonies and inadvertently had been bred to homozygosity (23, 24). This mutation complicates interpretation of the relationship between type I IFN and IRF5 expression and activation because $Dock2^{-/-}$ mice have independent immune system defects, including effects on IFN induction (25–27). After the Dock2 loss-of-function mutation was corrected, plasmacytoid dendritic cells stimulated with TLR agonists or HSV *ex vivo* showed small defects in IFN-α production, more substantive reductions in IFN-β, and larger decreases in IL-6 and TNF-α levels (23, 24). However, pathogenesis studies or detailed analysis of cytokine production *in vivo* after viral infection has not been analyzed in these newly generated $Irf5^{-/-} \times Dock2^{wt/wt}$ mice.

To better define the antiviral and immunoregulatory function of IRF5 *in vivo*, we infected $Irf5^{-/-} \times Dock2^{wt/wt}$ mice with WNV in the present study. These mice were highly vulnerable to infection with WNV, with most $Irf5^{-/-} \times Dock2^{wt/wt}$ animals succumbing to disease. This increase in mortality was associated with enhanced viral replication in peripheral tissues as well as in the brain and spinal cord. The loss of IRF5 was associated with decreased levels of proinflammatory cytokines and immune cell activation with a relatively preserved type I IFN response. Overall, our studies indicate that IRF5 transcriptional activity has key functions in orchestrating the early immune response in the draining lymph node (DLN) after WNV infection.

MATERIALS AND METHODS

Viruses and cells. The WNV strain (3000.0259) was isolated in New York in 2000 and passaged once in C6/36 *Aedes albopictus* cells. Mice were inoculated subcutaneously in the footpad with 10^2 PFU of WNV diluted in Hanks balanced salt solution (HBSS) and 1% heat-inactivated fetal bovine serum (FBS). Virus titers in tissues were analyzed by plaque assay using Vero cells, as described previously (28).

Mice. C57BL/6J wild-type (WT) mice were commercially obtained from Jackson Laboratories. $Irf5^{-/-}$ mice (18) originally were a gift from T. Taniguchi (Tokyo, Japan) and obtained from I. Rifkin (Boston, MA) and K. Fitzgerald (Worcester, MA) and had been backcrossed eight generations. After detection of a homozygous *Dock2* mutation in this line, we backcrossed the line for an additional five generations and selected animals that were $Dock2^{wt/wt}$ using PCR-based genotyping (23). $Irf5^{fl/fl}$ mice (29) on a C57BL/6 background were a gift from P. Pitha (Baltimore, MD) and crossed to congenic CMV-Cre recombinase mice (Jackson Laboratories) to generate an independent gene deletion of IRF5. Deletion of the floxed region results in a frameshift mutation that creates a premature stop codon in exon 3 of the *Irf5* gene (29). All mice were housed in a pathogen-free mouse facility at the Washington University School of Medicine and experiments were performed in accordance with federal and university regulations. The protocols were approved by the Institutional Animal Care and Use Committee at the Washington University School of Medicine (assurance number A3381-01). Mice (9 to 10 weeks old) were inoculated subcutaneously via footpad injection with 10^2 PFU of WNV diluted in 50 μl of HBSS supplemented with 1% heat-inactivated FBS.

For immunization studies, a purified, H_2O_2-inactivated WNV-Kunjin vaccine (30) was used. WT and $Irf5^{-/-}$ mice were immunized subcutaneously in the footpad with H_2O_2-WNV-KUNV containing ~10^7 PFU equivalents/μg protein that was adjuvanted with Matrix M1 (10 μg/mouse; Novavax, Inc.) in phosphate-buffered saline (PBS). Serum samples were obtained on days 14 and 28, and mice were boosted on day 30. At day 60, a final serum sample was obtained, and bone marrow and splenocytes were harvested for long-lived plasma cell (LLPC) and memory B cell (MBC) analysis (see below).

The genotyping primers spanning the *Dock2* exon duplication were published recently (ln29.4F, 5′-GAC CTT ATG AGG TGG AAC CAC AAC C-3′; lnR22.3.1R, 5′-GAT CCA AAG ATT CCC TAC AGC TCC AC-3′) (24). Genotyping primers for an internal control gene (CD19) to confirm adequacy of DNA sample preparation also have been published (oIMR1589F, 5′-CCT CTC CCT GTC TCC TTC CT-3′; oIMR1590R, 5′-TGG TCT GAG ACA TTG ACA ATC A-3′) (24).

Measurement of viral burden. At specified time points (i.e., day 1, 2, 3, 4, 5, 6, 8, or 10) after WNV infection, serum was obtained by intracardiac heart puncture, followed by extensive perfusion (20 ml of PBS) and organ recovery. Organs were weighed, homogenized using a bead-beater apparatus, and titrated by plaque assay on Vero cells (28) or quantitative reverse transcription-PCR (qRT-PCR), as described previously (14).

Quantification of type I IFN activity. Levels of biologically active type I IFN were determined by using an encephalomyocarditis virus (EMCV)-based cytopathic effect bioassay performed in murine L929 cells as described previously (8). Serum samples were treated with citrate buffer (40 mM citric acid, 10 mM KCl, 135 mM NaCl [pH 3.0]) for 10 min and neutralized with medium containing 50 mM HEPES (pH 8.0). The amount of type I IFN per ml of serum was calculated from a standard curve using IFN-β (PBL InterferonSource).

Cytokine Bio-Plex assay. WT and $Irf5^{-/-}$ mice were infected with WNV, and at specified times blood and the draining popliteal lymph nodes (LNs) were collected. Serum was isolated, and an LN homogenate was prepared. Individual LNs were homogenized in 250 μl of PBS using a bead-beater apparatus. The Bio-Plex Pro assay was performed according to the manufacturer's protocol (Bio-Rad).

Flow cytometry analysis of LN and spleen cells. Popliteal LNs or spleens were dissected from naive or WNV-infected mice. Single-cell suspensions were generated in Dulbecco modified Eagle medium (DMEM) containing 10% FBS. After erythrocyte lysis with ACK buffer (0.15 M NH_4Cl, 10 mM $KHCO_3$, 0.1 mM Na_2EDTA [pH 7.2]), cells were counted by hemocytometry, washed with PBS supplemented with 1% FBS, and incubated with conjugated antibodies. The following antibodies (clone names are indicated in parentheses) against mouse antigens were purchased from BD Biosciences, eBioscience, or Biolegend: anti-CD3ε-Alexa Fluor 647 (145-2C11), anti-CD4-phycoerythrin (PE; RM4-5), anti-CD8α-Alexa Fluor 700 (53-6.7), anti-CD11b-PE.Cy7 (M1/70), anti-CD11c-BD Horizon V450 (HL3), anti-CD19-PE.Texas Red (1D3), anti-CD69-Brilliant Violet 605 (H1.2F3), anti-NK1.1-PE (PK136), anti-Ly6G-PerCP.Cy5.5 (1A8), anti-MHC-II-APC.Cy7 (I-A/I-E; M5/114.15.2), anti-F4/80-fluorescein isothiocyanate (FITC; BM8), and fixable viability dye Efluor 506. Cells were stained in PBS with 1% FBS supplemented with Fc block (anti-CD16/32) to mini-

mize nonspecific binding, and appropriate isotype control antibodies purchased from Becton Dickinson Biosciences were used. The data were collected on a LSRII flow cytometer and analyzed using FlowJo software (Treestar, Inc.).

qRT-PCR. WT or *Irf5*$^{-/-}$ mice were infected with WNV, and draining popliteal LNs were harvested 2 days later. Total RNA was extracted by using an RNeasy kit (Qiagen). Fluorogenic qRT-PCR was performed using One-Step RT-PCR master mix and a 7500 Fast real-time PCR system (Applied Biosystems) with published TaqMan primers and probes (14). Gene induction was normalized to 18S rRNA levels.

B cell and antibody responses. The levels of WNV-specific IgM and IgG (including IgG1, IgG2b, IgG2c, and IgG3) were determined using an enzyme-linked immunosorbent assay (ELISA) against purified WNV E protein, as described previously (31). Focus reduction neutralization assays on Vero cells were performed after mixing serial dilutions of serum with a fixed amount (50 FFU) of WNV as previously described (32).

Enzyme-linked immunospot (ELISPOT) assays to determine the number of antigen-specific LLPCs were performed as described previously (33). Briefly, mixed cellulose filter plates (Millipore) were coated with 20 μg of recombinant WNV E protein/ml in PBS overnight at 4°C. The plates were washed twice with PBS with 0.1% Tween 20, washed twice with PBS, and blocked for 1 h at room temperature with DMEM supplemented with 10% FBS, penicillin-streptomycin, 10 mM HEPES, 50 μM β-mercaptoethanol, and 10 mM nonessential amino acids. Bone marrow cells from immunized mice were depleted of erythrocytes using ACK lysis buffer. Cells were resuspended at 2×10^6 cells/ml and serially diluted into wells. After 8 h at 37°C, the plates were washed extensively and incubated with 1 μg/ml biotinylated anti-IgG (Sigma-Aldrich) and then incubated overnight at 4°C. After washing, the wells were incubated with 1 μg/ml streptavidin conjugated to HRP diluted in PBS, 0.05% Tween 20, and 1% FBS. The plates were washed, and spots were developed using a chromogen substrate (AEC [3-amino-9 ethyl-carbazole]; Sigma-Aldrich). Spots were enumerated using a Biospot Analyzer (Cellular Technology, Ltd.).

WNV-specific MBC frequencies were determined as described previously (33) by measuring the reactivity of supernatants to recombinant WNV E protein by limiting dilution analysis (LDA) and ELISA. Splenocyte suspensions were generated from immunized mice. Erythrocytes were lysed (ACK lysis buffer; Invitrogen), and CD19$^+$ B cells were isolated by positive selection using magnetic beads (Miltenyi Biotec). B cells were resuspended in LDA medium (RPMI 1640, 10% FBS, penicillin-streptomycin, 1 mM sodium pyruvate, 0.1 mM nonessential amino acids, 10 mM HEPES, and 50 μM β-mercaptoethanol). B cells were cultured in 2-fold serial dilutions starting at 200,000 cells per well in 96-well flat-bottom plates on top of 20,000 3T3 transgenic feeder cells expressing BAFF and CD40L and treated with 5 μg/ml mitomycin C. Plates were incubated at 37°C and 5% humidified CO_2 for 6 days. To calculate the frequency of WNV-specific MBC that produced IgG, 96-well ELISA plates were coated with 5 μg/ml WNV E protein overnight at 4°C. The plates were washed and blocked with PBS–0.05% Tween 20 supplemented with 2% (wt/vol) bovine serum albumin for 1 h at 37°C. Supernatants from LDA plates were added to the ELISA plates (50 μl per well), and detection of WNV-specific antibody was performed as described for the ELISPOT assay. Positive wells were defined as wells that scored 2-fold over the mean optical density of negative-control wells (wells containing feeder cells alone). Supernatant from cultured naive splenocytes did not score positive.

Cellular immune responses. WT and *Irf5*$^{-/-}$ mice were infected subcutaneously in the footpad with 10^2 PFU of WNV and, at 8 days after infection, the spleens and brains were harvested after extensive cardiac perfusion with PBS. Splenocytes were dispersed into single cell suspensions with a cell strainer. Brains were minced and digested with 0.05% collagenase D, 0.1 μg/ml trypsin inhibitor TLCK, and 10 μg/ml DNase I in HBSS supplemented with 10 mM HEPES (pH 7.4; Life Technologies). Cells were dispersed into single cell suspensions with a cell strainer and pelleted through a 30% Percoll cushion for 30 min (1,200 × *g* at 4°C). Intracellular IFN-γ staining was performed after *ex vivo* restimulation with a D^b-restricted NS4B immunodominant peptide using 1 μM peptide and 5 μg/ml brefeldin A (Sigma) as described previously (34). Cells were stained with the following antibodies and processed on an LSR II flow cytometer (Becton Dickinson): CD3 (Becton Dickinson, clone 145-2C11), CD4 (Biolegend, clone RM4-5), CD8β (Biolegend, clone YT5156.7.7), CD45 (Biolegend, clone 30-F11), CD11b (Becton Dickinson, clone M1/70), CD11c (Becton Dickinson, clone HL3) MHC-II (Biolegend, clone M5/114.15.2), CD43 (Biolegend, clone IM7), and IFN-γ (Becton Dickinson, clone XMG1.2). Flow cytometry data were analyzed using FlowJo software (Treestar).

Data analysis. All data were analyzed using Prism software (GraphPad6, San Diego, CA). Kaplan-Meier survival curves were analyzed by the log-rank test. Differences in viral burden, cytokine levels, and cell numbers were analyzed by the Mann-Whitney test.

RESULTS

Susceptibility of Irf5-deficient mice to WNV infection. Given that prior viral pathogenesis studies may have used *Irf5*$^{-/-}$ mice containing a mutation in the *Dock2* gene, we confirmed that our backcrossed *Irf5*$^{-/-}$ strain had the WT *Dock2* allele (Fig. 1A). To determine whether IRF5 was required for restricting WNV pathogenesis *in vivo*, we infected 9- to 10-week-old WT and *Irf5*$^{-/-}$ × *Dock2*$^{wt/wt}$ (here called *Irf5*$^{-/-}$) mice with 10^2 PFU of WNV (New York 2000 strain) by subcutaneous inoculation and monitored survival over time. *Irf5*$^{-/-}$ mice exhibited enhanced mortality (81% versus 22%, $P < 0.0001$, Fig. 1B) and reduced average survival time (mean time to death: 10.5 and 12.2 days for *Irf5*$^{-/-}$ and WT mice, respectively, $P < 0.01$) compared to WT mice.

To begin to determine the basis for the increased lethality in *Irf5*$^{-/-}$ mice after WNV infection, we measured viral loads in tissues at different time points. An absence of IRF5 resulted in enhanced viremia (9- to 10-fold at days 2 and 4 after infection, $P < 0.05$; Fig. 1C) and increased WNV infection in the spleen (31-fold at day 4, $P < 0.01$; Fig. 1D). A small effect was observed in the kidney at day 4, since 5 of 11 *Irf5*$^{-/-}$ mice had measurable infectious WNV compared to 0 of 10 WT mice (Fig. 1E).

Higher levels of WNV infection also were observed in central nervous systems (CNS) of *Irf5*$^{-/-}$ mice compared to WT controls. At day 4 after infection, 4 of 11 *Irf5*$^{-/-}$ mice had measurable viral loads in the brain compared to 0 of 7 WT mice (Fig. 1F). Analogously, 5 of 10 *Irf5*$^{-/-}$ mice had detectable WNV in the spinal cord at day 6 compared to 0 of 10 WT mice (Fig. 1G). This pattern resulted in increased titers at later times in the brain (22- to 145-fold increase at days 6, 8, and 10, $P < 0.01$) and spinal cord (38-fold at day 10, $P < 0.01$) of *Irf5*$^{-/-}$ mice. At day 9 after infection, higher levels of WNV were detected in several different regions of the brain, including the cerebellum, cerebral cortex, brain stem, white matter, and olfactory bulb (Fig. 1J to N, $P < 0.05$).

To corroborate these results, we crossed *Irf5*$^{fl/fl}$ mice (29) to a congenic CMV-Cre recombinase strain to generate an independent line with a targeted deletion of IRF5. Analogous to the data obtained with *Irf5*$^{-/-}$ mice, 9-week-old CMV-Cre *Irf5*$^{fl/fl}$ mice succumbed to WNV infection at a greater rate than age-matched control Cre-negative *Irf5*$^{fl/fl}$ mice (89% versus 25%, $P < 0.002$, Fig. 1H) and exhibited a higher viremia (8-fold at day 4 after infection, $P < 0.04$; Fig. 1I).

Because previous studies showed antiviral effects of the TLR and RLR signaling pathways in resident cells of the CNS (12, 35–37), we hypothesized that part of the enhanced WNV infection phenotype in *Irf5*$^{-/-}$ mice could be explained by an IRF5-dependent restriction of replication in resident neuronal cells or micro-

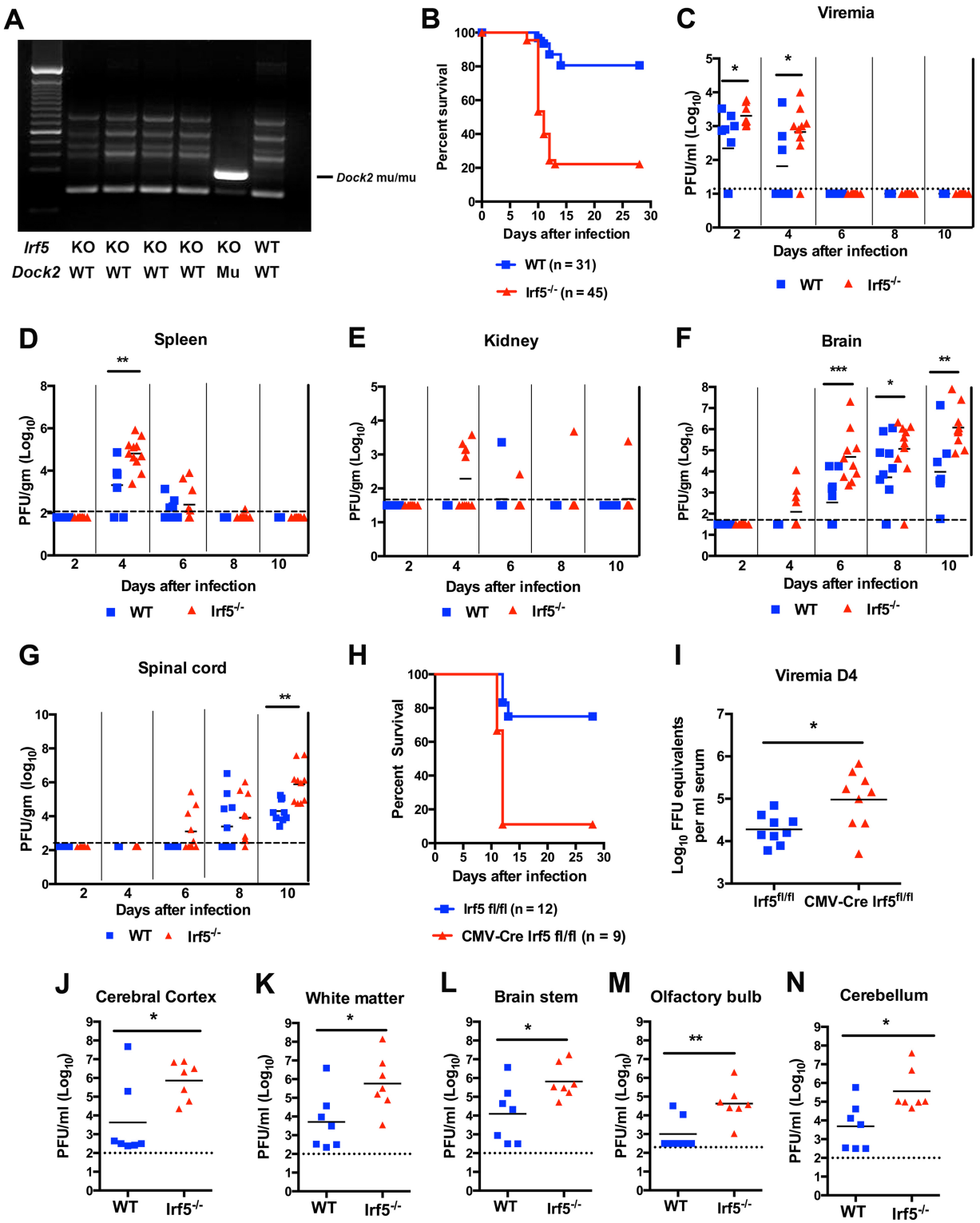

FIG 1 Survival and viral burden in WT and $Irf5^{-/-}$ mice after peripheral inoculation of WNV. (A) Dock2 gene PCR results from genotyping of WT, $Irf5^{-/-} \times Dock2^{mu/mu}$, and $Irf5^{-/-} \times Dock2^{wt/wt}$ mice with primers amplifying the region flanking the duplication. A 305-bp amplicon that spans the genomic duplication of $Dock2^{mu/mu}$ is observed only in the parent $Irf5^{-/-}$ mice prior to backcrossing. It is not amplified in the new $Irf5^{-/-} \times Dock2^{wt/wt}$ mice. Note, the other sized bands are nonspecific amplification products. (B) $Irf5^{-/-} \times Dock2^{wt/wt}$ (herein referred to as $Irf5^{-/-}$) mice were infected with 10^2 PFU of WNV in the footpad. Survival was monitored for 30 days: $n = 31$ WT and 45 $Irf5^{-/-}$ mice from at least three independent experiments. The difference was statistically different ($P < 0.0001$), as judged by the log-rank test. (C to G) The viral burdens after WNV infection of WT and $Irf5^{-/-}$ mice were measured by plaque assay in samples from serum (C), spleen (D), kidney (E), brain (F), and spinal cord (G). A scatter plot of data is shown with each individual point

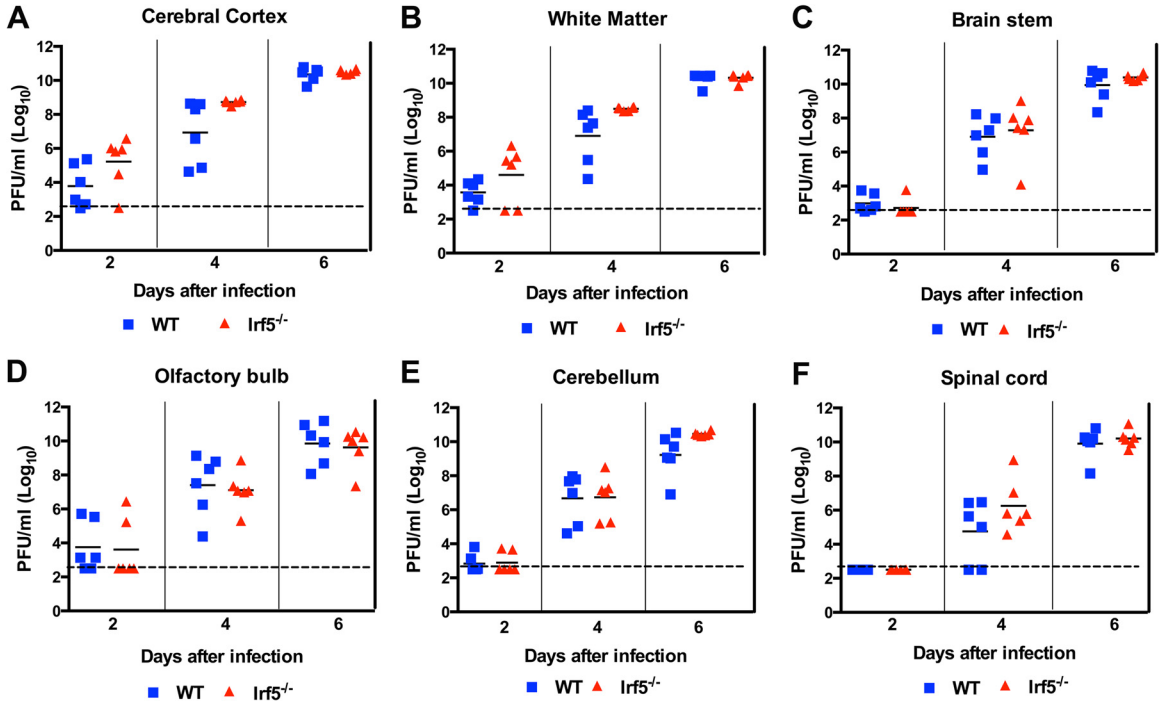

FIG 2 Viral replication in CNS tissues of WT and *Irf5*$^{-/-}$ mice after intracranial infection. (A to F) Mice were infected with 10^1 PFU of WNV by intracranial injection. Viral replication was measured in the cerebral cortex (A), white matter (B), brain stem (C), olfactory bulb (D), cerebellum (E), and spinal cord (F) by plaque assay from 2 to 6 days after infection. A scatter plot of the data is shown, with each individual point representing a single animal. The bars indicate mean values and were obtained from six mice per time point. The dashed lines represent the limit of sensitivity of the assay. None of the differences between WT and *Irf5*$^{-/-}$ mice were statistically significant, as judged by the Mann-Whitney test.

glia. To test this, WT and *Irf5*$^{-/-}$ mice were infected with 10^1 PFU of WNV directly into the brain via an intracranial route, and viral burden in the cerebral cortex, white matter, brain stem, cerebellum, and spinal cord was measured on days 2, 4, and 6 after infection. In contrast to the increased virus titers observed in the CNS of *Irf5*$^{-/-}$ mice after peripheral inoculation, we observed no significant differences in infection between WT and *Irf5*$^{-/-}$ mice following intracranial injection (Fig. 2A to E, $P > 0.05$). These data show that IRF5 is not required to restrict WNV replication directly in the CNS. More likely, the increased WNV titers in the CNS after subcutaneous inoculation reflect the enhanced infection in peripheral organs, which results in dissemination to the CNS prior to evolution of a protective adaptive immune response.

Effect of IRF5 on innate immune responses. Since IRF5 has been reported to be required for an optimal type I IFN response *in vivo* in the context of VSV, HSV, and NDV infections (20, 21), we assessed its impact on the systemic levels of type I IFN after WNV infection (Fig. 3A). However, we observed no significant difference in type I IFN levels in the serum of *Irf5*$^{-/-}$ mice using a sensitive EMCV-based bioassay in L929 cells at days 1, 2, or 4 after infection. A small, yet statistically significant decrease in type I IFN levels was observed in the serum of *Irf5*$^{-/-}$ mice at day 3 after infection.

We assessed the role of IRF5 on systemic production of other cytokines and chemokines at 1, 2, or 4 days after WNV infection (Fig. 3B to G). Notably, serum levels of IL-6, IL-10, IL-12p40, macrophage inflammatory protein 1α (MIP-1α; CCL3), MIP-1β (CCL4), and macrophage chemoattractant protein 1 (MCP-1; CCL2) were lower in serum within the first 2 days of WNV infection in *Irf5*$^{-/-}$ compared to WT mice. By day 4, however, differences in these cytokine and chemokine levels in serum were largely absent, indicating that IRF5-independent pathways could compensate for their production. In comparison, levels of other inflammatory cytokines and chemokines (IFN-γ, TNF-α, IL-1β, and RANTES [CCL5]) were similar in WT and *Irf5*$^{-/-}$ mice (data not shown). Overall, these results consistently show small defects in the early serum inflammatory cytokine and chemokine response of WNV-infected *Irf5*$^{-/-}$ mice and extend results observed previously with VSV, HSV, or NDV infection (20, 21).

Because the differences in serum levels of proinflammatory

representing a single animal. The bars indicate mean values and were obtained from 7 to 11 mice per time point. The dashed lines represent the limit of sensitivity of the assay. Asterisks indicate statistical significance (*, $P < 0.05$; **, $P < 0.01$; ***, $P < 0.001$), as judged by the Mann-Whitney test. (H and I) CMV-Cre *Irf5*$^{fl/fl}$ and control *Irf5*$^{fl/fl}$ (Cre-negative) mice were infected with 10^2 PFU of WNV in the footpad. (H) Survival was monitored for 30 days: $n = 9$ CMV-Cre *Irf5*$^{fl/fl}$ and 12 *Irf5*$^{fl/fl}$ mice from at least three independent experiments. The difference was statistically different ($P < 0.002$), as judged by a log-rank test. (I) Viremia was assessed by qRT-PCR at day 4 after WNV infection in CMV-Cre *Irf5*$^{fl/fl}$ and control *Irf5*$^{fl/fl}$ (Cre-negative) mice and expressed as focus-forming unit (FFU) equivalents after comparison to a standard curve. The bars indicate mean values and were obtained from nine mice per group. The difference was statistically significant (*, $P < 0.05$), as judged by the Mann-Whitney test. (J to N) Viral burdens in the cerebral cortex (I), cortical white matter (J), brain stem (K), olfactory bulb (L) and cerebellum (M) in the brains of WT and *Irf5*$^{-/-}$ mice on day 9 after subcutaneous WNV infection. The samples ($n = 7$) were analyzed as described in panels D to H.

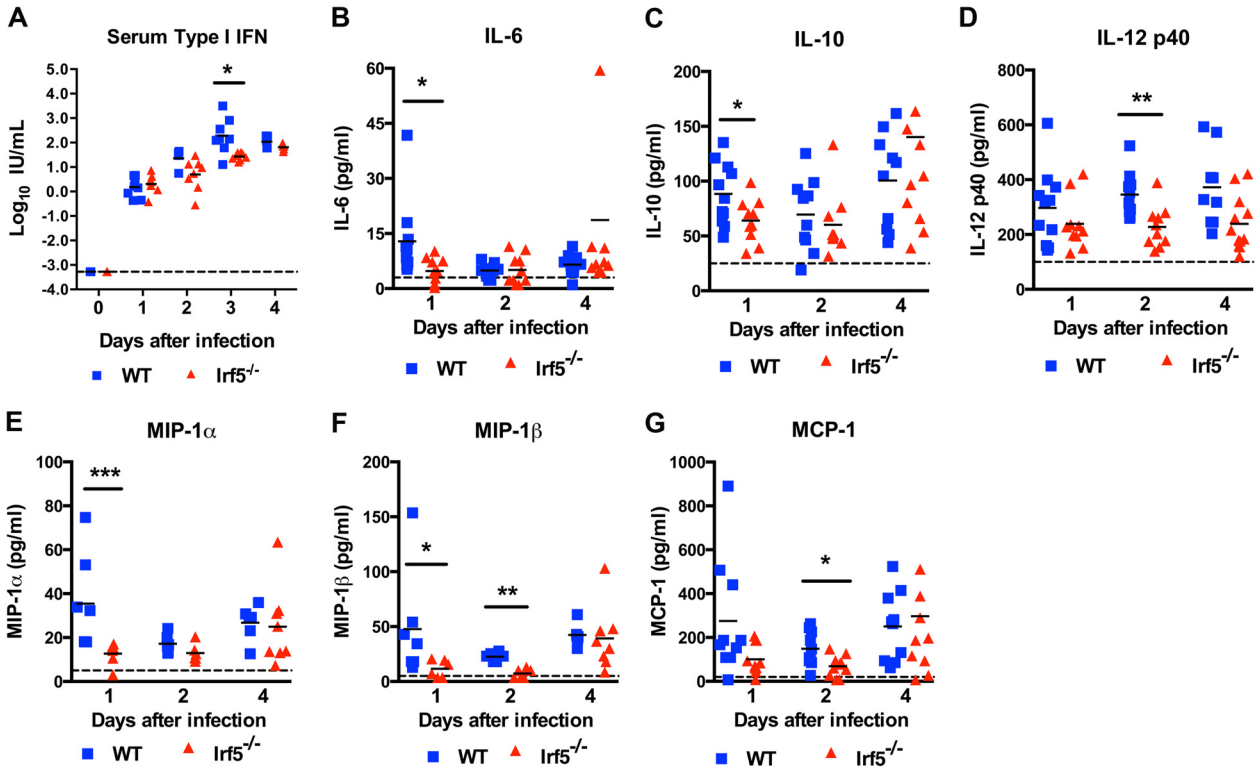

FIG 3 Systemic cytokine and chemokine responses after WNV infection of WT and *Irf5*$^{-/-}$ mice. Mice were infected with 10^2 PFU of WNV in the footpad, and serum was harvested at days 1, 2, 3, or 4 after infection. (A) The type I IFN activity in serum of WT and *Irf5*$^{-/-}$ mice was measured by an EMCV cytopathic effect bioassay. (B to G) Cytokine and chemokine levels in the sera of WNV-infected WT and *Irf5*$^{-/-}$ mice were measured by Bio-Plex assay. The data are presented as scatter plots from 6 to 10 mice per group. Bars represent the means, and dotted lines indicate the limit of sensitivity of each assay. Asterisks indicate statistical significance (*, $P < 0.05$; **, $P < 0.01$; ***, $P < 0.001$), as judged by the Mann-Whitney test.

cytokines between WT and *Irf5*$^{-/-}$ mice occurred early after infection, we speculated this might reflect events occurring in the draining popliteal LN (DLN), an initial site of WNV replication and innate immune response after subcutaneous footpad inoculation (38). We first compared levels of viral RNA in the DLN in WT and *Irf5*$^{-/-}$ mice. Notably, at day 2 after infection, no difference in WNV infection was observed in the two groups of mice ($P > 0.7$, Fig. 4A). We next measured the levels of cytokines and chemokines in homogenates prepared from DLN of WNV-infected WT and *Irf5*$^{-/-}$ mice. The levels of 11 different cytokines and chemokines were consistently lower in WNV-infected *Irf5*$^{-/-}$ mice compared to WT mice (Fig. 4B to L). In comparison, the mRNA levels of *IFN*β, *IFN*α, and two ISGs (*Rsad2* and *Oas1*) were minimally different in DLN samples from WT and *Irf5*$^{-/-}$ mice (Fig. 4M).

While measuring cytokine and chemokine levels in DLN homogenates, we noticed the DLN from WNV-infected *Irf5*$^{-/-}$ mice were smaller in size in comparison to their WT counterparts (data not shown). We explored this by assessing whether a deficiency of IRF5 affected the number and activation state of immune cell subsets. In the popliteal LN of *Irf5*$^{-/-}$ naive mice, we measured 1.5- to 4-fold fewer cells in several leukocyte subsets, with the differences in NK cells and macrophages attaining statistical significance (Table 1). By day 2 after WNV infection, we observed 2- to 3-fold fewer B cells, CD4$^+$ T cells, CD8$^+$ T cells, NK cells, F4/80$^+$ macrophages, and CD11c$^+$ dendritic cells (Fig. 5A to F, $P < 0.05$) in the DLN of WNV-infected *Irf5*$^{-/-}$ mice compared to WT mice. No difference in the numbers of Ly6G$^+$ neutrophils was detected in the DLN at this time point (data not shown). Moreover, B cells, CD4$^+$ T cells, and CD8$^+$ T cells from *Irf5*$^{-/-}$ mice expressed the activation marker CD69 on their surface at a lower frequency ($P < 0.001$, Fig. 5G to I), and *Irf5*$^{-/-}$ macrophages expressed lower level of class II major histocompatibility complex (MHC) antigen ($P < 0.001$, Fig. 5K) than did cells from WT mice. Because of the differences in cellularity of the LNs in *Irf5*$^{-/-}$ mice, we performed a similar analysis of splenocyte subsets in naive and WNV-infected animals. In contrast to the differences observed in the LN, in the spleen we did not detect a difference in the number B cells, CD4$^+$ T cells, CD8$^+$ T cells, NK cells, dendritic cells, or granulocytes in WT and *Irf5*$^{-/-}$ mice at baseline or 2 days after WNV infection (Tables 1 and 2). Collectively, these experiments suggest that IRF5 has a key role in shaping the early innate cellular immune response in the DLN after subcutaneous infection with WNV.

Effect of IRF5 on adaptive cellular immune responses. Prior studies revealed that an optimal T cell response to WNV requires MAVS signaling (12) and that IRF5-dependent transcription in dendritic cells is regulated in part by MAVS-dependent signaling events (14). Given these findings and our current results showing that *Irf5*$^{-/-}$ mice had lower levels of proinflammatory cytokines in the DLN and higher levels of WNV infection in organs that are cleared by effector T cells (39–42), we evaluated whether defects in cellular immune responses in peripheral tissues or the brain in

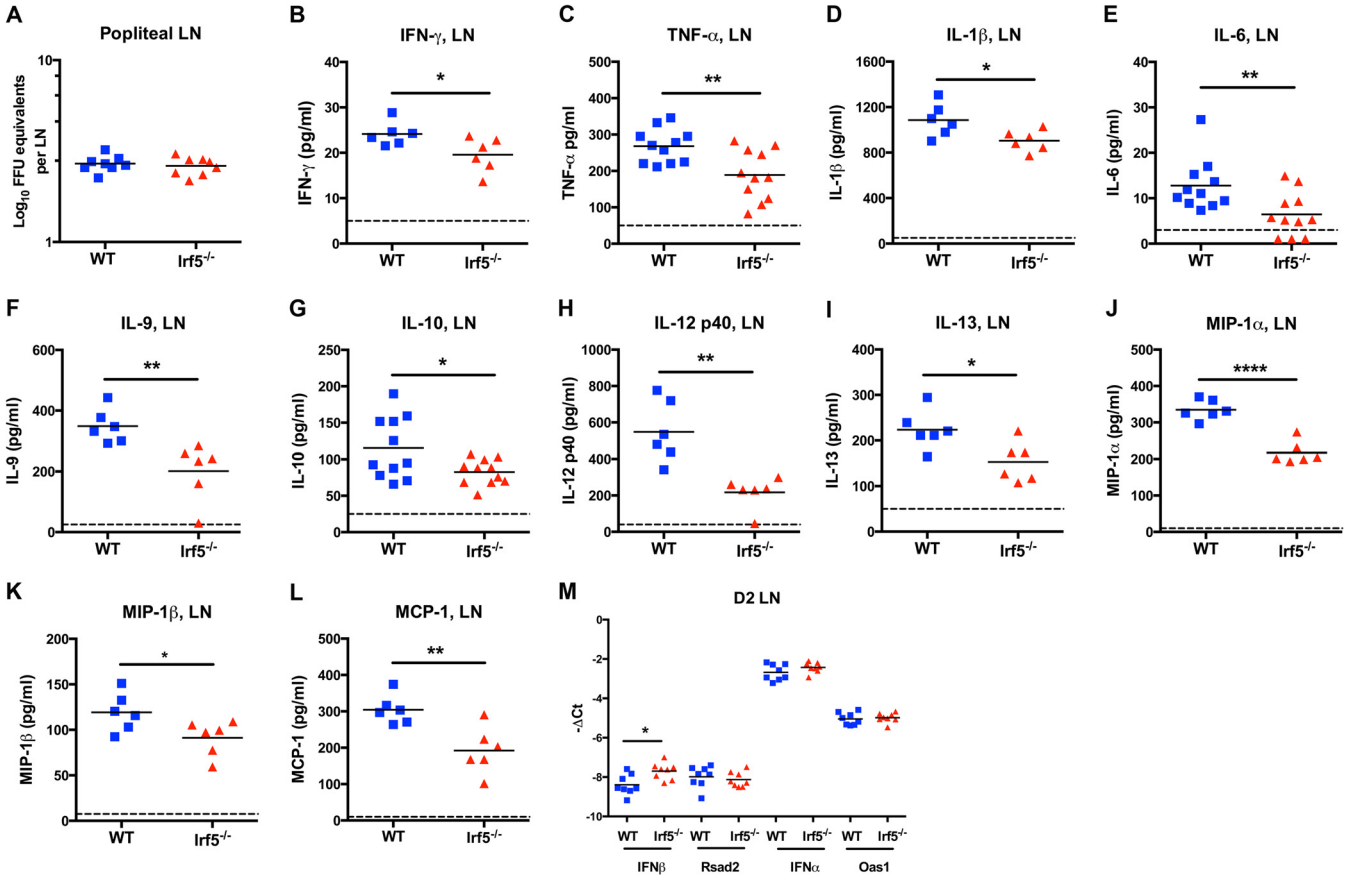

FIG 4 Cytokine and chemokine responses in the draining popliteal LNs after WNV infection of WT and *Irf5*$^{-/-}$ mice. Mice were infected bilaterally with 10^2 PFU of WNV in the footpad, and LNs were harvested at day 2 after infection. (A) Levels of viral infection in LN homogenates as measured by qRT-PCR. The differences were not statistically different as measured by the Mann-Whitney test. (B to L) Cytokine and chemokine levels in LN of WNV-infected WT and *Irf5*$^{-/-}$ mice were measured by a Bio-Plex assay. The data are presented as scatter plots from 6 to 11 independent measurements, reflecting a total of 12 to 22 LNs over three or four independent experiments for each genotype. Bars represent the mean and dotted lines indicate the limit of sensitivity of each assay. (M) Expression of the indicated IFNs and ISG in the DLN was measured from total RNA 2 days after WNV infection of WT and *Irf5*$^{-/-}$ mice by qRT-PCR. Gene expression was compared to levels of 18S rRNA in the sample and displayed as the ΔC_T value. The data represent the averages from eight samples from two independent experiments. In this figure, asterisks indicate statistical significance (*, $P < 0.05$; **, $P < 0.01$; ****, $P < 0.0001$) as judged by the Mann-Whitney test.

Irf5$^{-/-}$ mice contributed to the susceptibility phenotype after WNV infection.

We initially harvested splenocytes from WT and *Irf5*$^{-/-}$ mice at 6 days after WNV infection, a relatively early time point in the evolution of the cellular response, and performed immunophenotyping analysis. Cells were stained with D^b-NS4B peptide tetramers to establish antigen specificity and antibodies to granzyme B to monitor effector function (Fig. 6A to C). No significant difference in the percentage of number of NS4B-tetramer positive cells expressing Granzyme B in WNV-infected WT and *Irf5*$^{-/-}$ mice was detected at day 6 ($P > 0.1$). We also analyzed the cellular response in the spleen at a later time, day 8 after infection. Cells were stained with antibodies to detect T cells (CD3, CD4, and CD8) and the production of effector molecules (IFN-γ) after WNV peptide restimulation and to detect D^b-NS4B peptide tetramers. Again, we observed no significant differences in the percentage or total number of CD4$^+$ or CD8$^+$ T cells (Fig. 6D and E, $P > 0.4$) or antigen-specific tetramer-positive CD8$^+$ T cells (Fig. 6F and G, $P > 0.7$) in the spleens of WNV-infected WT and *Irf5*$^{-/-}$ mice. Consistent with this, after *ex vivo* peptide restimulation, we detected no difference in the percentages or numbers of CD8$^+$ T cells producing IFN-γ (Fig. 6H and I, $P > 0.5$) or TNF-α (data not shown).

Although T cell responses were intact in the spleens from *Irf5*$^{-/-}$ mice, it remained possible that the viral burden phenotype in the CNS was due, in part, to impaired immune cell trafficking across the blood-brain barrier or altered function of cells within the CNS. To address this, we analyzed immune cell accumulation in the brain at day 8 after WNV infection. We observed no difference in the percentages or numbers of NS4B-specific CD8$^+$ T cells (Fig. 7A and B, $P > 0.2$) or IFN-γ-producing CD8$^+$ T cells after peptide restimulation (Fig. 7C and D, $P > 0.2$) in the brain. Analogously, the percentages or numbers of CD11b$^+$CD45^{lo} microglia or infiltrating CD11b$^+$CD45^{hi} macrophages (Fig. 7E and F, $P > 0.2$) in the brains of WNV-infected WT and *Irf5*$^{-/-}$ mice were similar. Thus, the increased WNV titers observed in the CNS of *Irf5*$^{-/-}$ mice were not due to major defects in the generation or localization of antigen-specific T cells or other inflammatory cells.

Effect of IRF5 on humoral immune responses. Prior studies have suggested that IRF5 regulates Ikaros expression in B cells to generate an optimal class-switched antibody response to T-de-

TABLE 1 Number of cells in the naive popliteal LNs and spleens of WT and *Irf5*$^{-/-}$ mice[a]

Cell type	Mean no. of cells ± SD		*P*
	WT mice	*Irf5*$^{-/-}$ mice	
Lymph node			
CD19$^+$ B cells	$2.9 \times 10^5 \pm 8.9 \times 10^4$	$7.5 \times 10^4 \pm 3.7 \times 10^4$	0.07
CD4$^+$ T cells	$1.6 \times 10^5 \pm 2.7 \times 10^4$	$8.1 \times 10^4 \pm 4.2 \times 10^4$	0.13
CD8$^+$ T cells	$1.3 \times 10^5 \pm 2.3 \times 10^4$	$5.7 \times 10^4 \pm 2.8 \times 10^4$	0.11
NK1.1$^+$ NK cells	$4.8 \times 10^3 \pm 1.0 \times 10^3$	$1.2 \times 10^3 \pm 3.3 \times 10^2$	0.04
CD11b$^+$ F4/80$^+$ macrophages	$1.9 \times 10^3 \pm 9.9 \times 10^2$	$3.2 \times 10^2 \pm 1.7 \times 10^2$	0.02
CD11c$^+$ DCs	$1.1 \times 10^3 \pm 8.2 \times 10^2$	$1.9 \times 10^2 \pm 1.4 \times 10^2$	0.10
Lys6G$^+$ granulocytes	$9.0 \times 10^2 \pm 3.6 \times 10^2$	$2.6 \times 10^2 \pm 1.1 \times 10^2$	0.11
Spleen			
CD19$^+$ B cells	$2.6 \times 10^7 \pm 3.0 \times 10^6$	$2.7 \times 10^7 \pm 3.0 \times 10^6$	0.68
CD4$^+$ T cells	$9.7 \times 10^6 \pm 8.9 \times 10^5$	$1.1 \times 10^7 \pm 1.1 \times 10^6$	0.50
CD8$^+$ T cells	$5.9 \times 10^6 \pm 8.6 \times 10^5$	$6.7 \times 10^6 \pm 7.0 \times 10^5$	0.52
NK1.1$^+$ NK cells	$2.1 \times 10^6 \pm 2.6 \times 10^5$	$1.8 \times 10^6 \pm 2.1 \times 10^5$	0.57
CD11c$^+$ DCs	$5.3 \times 10^4 \pm 6.8 \times 10^3$	$7.7 \times 10^4 \pm 1.0 \times 10^4$	0.14
Lys6G$^+$ granulocytes	$5.6 \times 10^5 \pm 1.0 \times 10^5$	$1.5 \times 10^6 \pm 5.0 \times 10^5$	0.14

[a] Popliteal lymph node cells and splenocytes were collected from uninfected WT and *Irf5*$^{-/-}$ mice. Cells were phenotyped (see Materials and Methods) and processed by flow cytometry. The results are the averages from three to five mice per group. The groups were compared, and the indicated *P* values of <0.05 (Mann-Whitney test) reached statistical significance. DCs, dendritic cells.

pendent and -independent antigens (29) and that an absence of IRF5 alters B cell maturation (43), which prevents the development of antinuclear antibodies in a murine model of systemic lupus erythematosis (SLE) induced by pristine injection (44). Given that recent studies suggested that at least some of the cell-intrinsic B cell defects originally described could be due to the adventitious homozygous mutation of *Dock2* that was present in many *Irf5*$^{-/-}$ mouse colonies (23, 24), we analyzed humoral responses to WNV infection in our *Irf5*$^{-/-}$ mice, which have a WT *Dock2* allele. This analysis also was important because the B cell response to WNV is critical for controlling viremia and dissemination into the CNS (28, 32, 45).

To assess the effect of IRF5 on early WNV-specific antibody responses, we analyzed serum from *Irf5*$^{-/-}$ and WT mice 4 and 8 days after infection for binding to WNV E protein. At day 4, we observed a small decrease in the magnitude of the IgM response in *Irf5*$^{-/-}$ mice (2-fold, $P < 0.01$, Fig. 8A). By day 8, no difference was observed in the IgM response (Fig. 8B). At day 8, we also observed slightly lower levels (2-fold, $P < 0.01$, Fig. 8C) of WNV-specific IgG in *Irf5*$^{-/-}$ mice. However, this difference was subtle and did not impact the neutralizing capacity of serum (Fig. 8D).

One caveat to this analysis of the humoral response was that we observed 2-fold lower antibody titers in the setting of substantially increased viral replication, especially in the spleen (see Fig. 1D). In prior studies with mice deficient in IFN-γ (46), increased replication in peripheral organs was associated with higher antibody responses possibly secondary to the increased amount of viral antigen present. Thus, the higher level of antigen associated with enhanced infection of *Irf5*$^{-/-}$ mice could mask defects in the evolution of the humoral response. Given this possibility, and the prior studies suggesting a B cell intrinsic effect of IRF5 (29), we assessed anti-WNV B cell responses in WT and *Irf5*$^{-/-}$ mice after immunization with a nonreplicating H_2O_2-inactivated vaccine candidate (30). Mice were immunized with adjuvanted H_2O_2-inactivated WNV-Kunjin strain and boosted at day 30. One month later, the spleens and bone marrow were harvested for analysis of WNV-specific MBCs and long-lived plasma cells (LLPCs) by limiting dilution and ELISPOT analyses (33), respectively. Consistent with a role for IRF5 in optimal B cell responses (29), *Irf5*$^{-/-}$ mice had fewer WNV-specific MBCs and LLPCs at day 60 after initial vaccination (Fig. 8E and F). Lower titers of WNV-specific antibodies in serum also were observed in immunized *Irf5*$^{-/-}$ mice at day 60, 1 month after boosting (Fig. 8G). As reported previously (29), part of this defect reflected isotype skewing away from virus-specific antibodies of the IgG2c subtype (Fig. 8H). Similar to that seen with infectious WNV, the differences in serum and cellular antibody responses with nonreplicating inactivated virus between WT and *Irf5*$^{-/-}$ mice were reproducible yet relatively small. Although IRF5 contributes to an optimal humoral response, it is not required for its generation.

DISCUSSION

Although the roles of IRF3 and IRF7 in regulating IFN-dependent and IFN-independent antiviral responses are well established, the significance of the transcription factor IRF5 in this response has remained less certain, in part due to variation in results obtained from different groups with *Irf5*$^{-/-}$ mice. One explanation for these conflicting results was the recent discovery of a spontaneous genomic duplication and frameshift mutation in the guanine exchange factor *Dock2* that had arisen spontaneously in several colonies of *Irf5*$^{-/-}$ mice and inadvertently been bred to homozygosity (23, 24). Because *Dock2*-deficient mice have independent immune system defects, including effects on type I IFN induction (25–27), the relationship between IRF5 expression, type I IFN production, and viral pathogenesis required reassessment. In more recent studies, we used *Irf3*$^{-/-}$ × *Irf7*$^{-/-}$ DKO mice and *Irf3*$^{-/-}$ × *Irf5*$^{-/-}$ × *Irf7*$^{-/-}$ TKO mice to assess whether IRF5 was a possible source of the residual induction of IFN-β and ISGs in dendritic cells (14). These experiments suggested that, in the absence of the transcription factors IRF3 and IRF7, IRF5 was responsible for mediating the type I IFN and ISG response after WNV infection. However, these studies did not explore the nonredundant functions of IRF5 and their effects on restriction of virus infection.

Here, using *Irf5*$^{-/-}$ mice with WT *Dock2* alleles, we established a protective role for IRF5 in the context of WNV infection. These results were corroborated with CMV-Cre *Irf5*$^{fl/fl}$ mice, an independently generated mouse line with a targeted deletion of IRF5. An absence of IRF5 *in vivo* resulted in increased lethality and higher viral loads in the CNS compared to WT mice. Detailed virological and immunological analyses revealed that IRF5 contributed to the control of WNV at the earliest stages, since infection was increased in the blood and the spleen within a few days of inoculation, which ultimately resulted in enhanced replication in the brain and spinal cord. IRF5 had a subordinate role in the induction of type I IFN since relatively minor defects in the serum or DLN levels were detected in WNV-infected *Irf5*$^{-/-}$ mice. In comparison, mice lacking IRF5 showed blunted production of proinflammatory cytokines and chemokines at early time points, which was associated with fewer immune cells being recruited to the DLN. Vaccination and infection studies in *Irf5*$^{-/-}$ mice also

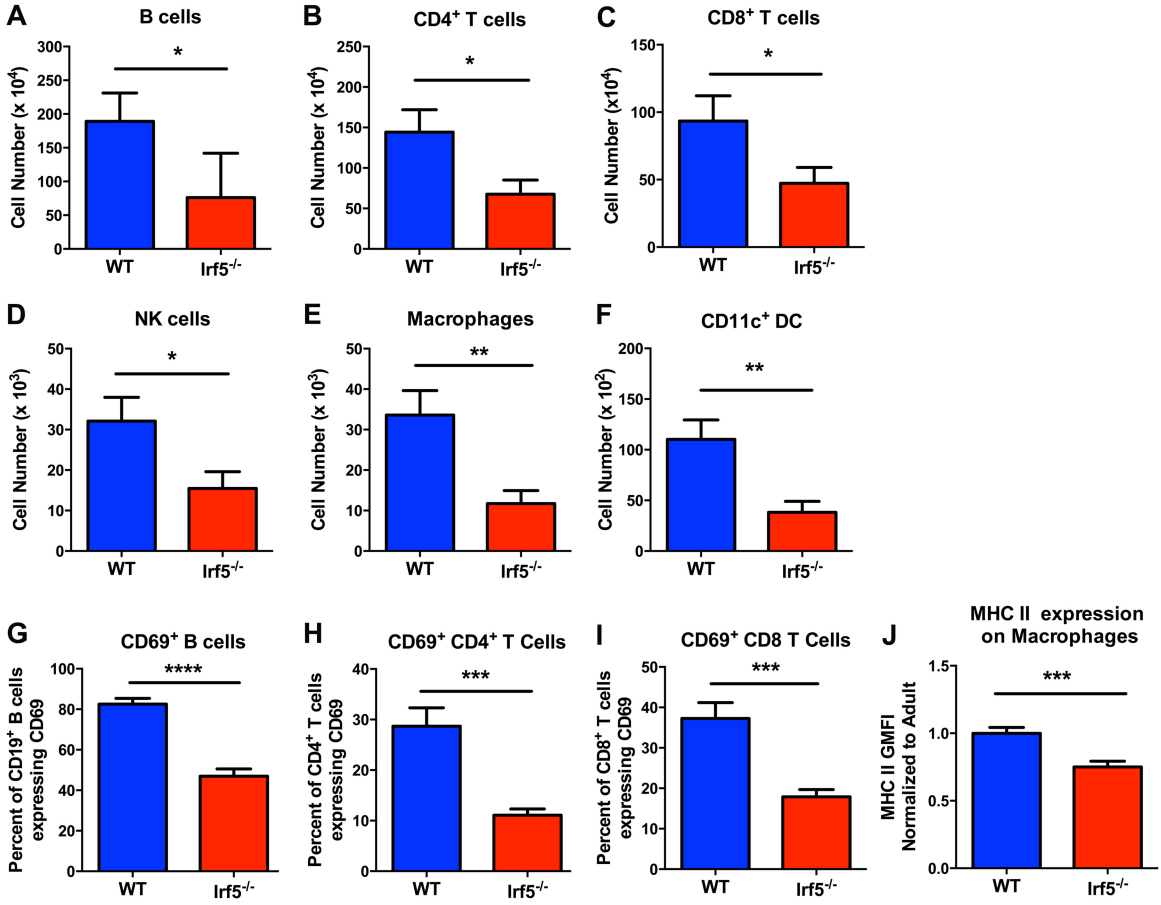

FIG 5 Leukocyte infiltration and activation in popliteal LNs of WNV-infected WT and *Irf5*$^{-/-}$ mice. WT and *Irf5*$^{-/-}$ mice were infected with 10^2 PFU of WNV in the footpad. Two days later, the draining popliteal LNs were harvested, and the cells were counted and stained with monoclonal antibodies to detect specific cell populations, including CD19$^+$ B cells (A), CD4$^+$ T cells (B), CD8$^+$ T cells (C), NK1.1$^+$ NK cells (D), CD11b$^+$ F4/80$^+$ macrophages (E), and CD11c$^+$ dendritic cells (F). B cells (G) and T cells (H and I) were costained with MAbs to CD69 and macrophages were stained with MAbs to class II MHC (MHC II) (J) to establish activation state. The results are the pooled from two independent experiments with a total of 9 to 10 mice per group, and bars indicate the standard errors of the mean. Asterisks indicate statistical significance as judged by the Mann-Whitney test (*, $P < 0.05$; **, $P < 0.01$; ***, $P < 0.001$; ****, $P < 0.0001$).

revealed defects in the generation of an optimal acute and memory B cell response, although the antigen-specific CD8$^+$ T cell response remained preserved. Collectively, our results suggest that the nonredundant role of IRF5 is primarily immunomodulatory, since its transcriptional activity shapes the magnitude, composition, and activation state of cellular infiltrates in lymphoid tissues.

TABLE 2 Number of immune cells in the spleens of WT and *Irf5*$^{-/-}$ mice at day 2 after WNV infection[a]

Cell type	Mean no. of cells ± SD		*P*
	WT mice	*Irf5*$^{-/-}$ mice	
CD19$^+$ B cells	$2.2 \times 10^7 \pm 2.0 \times 10^6$	$2.3 \times 10^7 \pm 2.1 \times 10^{46}$	0.67
CD4$^+$ T cells	$9.2 \times 10^6 \pm 1.0 \times 10^6$	$1.1 \times 10^7 \pm 7.8 \times 10^5$	0.25
CD8$^+$ T cells	$5.8 \times 10^6 + 5.7 \times 10^5$	$6.4 \times 10^6 \pm 2.9 \times 10^5$	0.20
NK1.1$^+$ NK cells	$1.7 \times 10^6 \pm 2.1 \times 10^5$	$1.8 \times 10^6 \pm 2.1 \times 10^5$	0.91
CD11c$^+$ DCs	$4.2 \times 10^4 \pm 7.5 \times 10^3$	$6.5 \times 10^4 \pm 1.0 \times 10^4$	0.07
Lys6G$^+$ granulocytes	$6.2 \times 10^5 \pm 1.7 \times 10^5$	$1.0 \times 10^6 \pm 4.8 \times 10^5$	0.43

[a] Splenocytes were collected from WT and *Irf5*$^{-/-}$ mice 2 days after WNV infection. Cells were phenotyped (see Materials and Methods) and processed by flow cytometry. The results are the averages from five to seven mice per group. None of the differences between groups attained statistical significance ($P > 0.05$). DCs, dendritic cells.

This activity modulates the early antiviral response and the transition to adaptive immunity, especially in the B cell compartment.

Our experiments suggest that *in vivo*, IRF5 does not have a major nonredundant role in regulating systemic type I IFN production, at least after WNV infection. These data are consistent with the original characterization of *Irf5*$^{-/-}$ mice (18) in which defects in proinflammatory cytokine production but not IFN-α production were observed after the treatment of dendritic cells or animals with TLR agonists. These results vary with those reported after infection with other viruses, which showed reduced levels of IFN-α and IFN-β in serum of infected *Irf5*$^{-/-}$ mice (20, 21), although some of the differences were small and did not attain statistical significance (20). While the basis for the discrepancy in nonredundant effects of IRF5 on the systemic type I IFN response warrants further analysis, there are at least two possible explanations. First, cell-type-specific effects of IRF5 in the context of infection by different viruses could impact the induction of type I IFN. In the context of NDV infection, an absence of IRF5 in cultured dendritic cells but not peritoneal macrophages was associated with reduced levels of type I IFN in the supernatant (20). *Irf5*$^{-/-}$ plasmacytoid dendritic cells obtained directly from mice

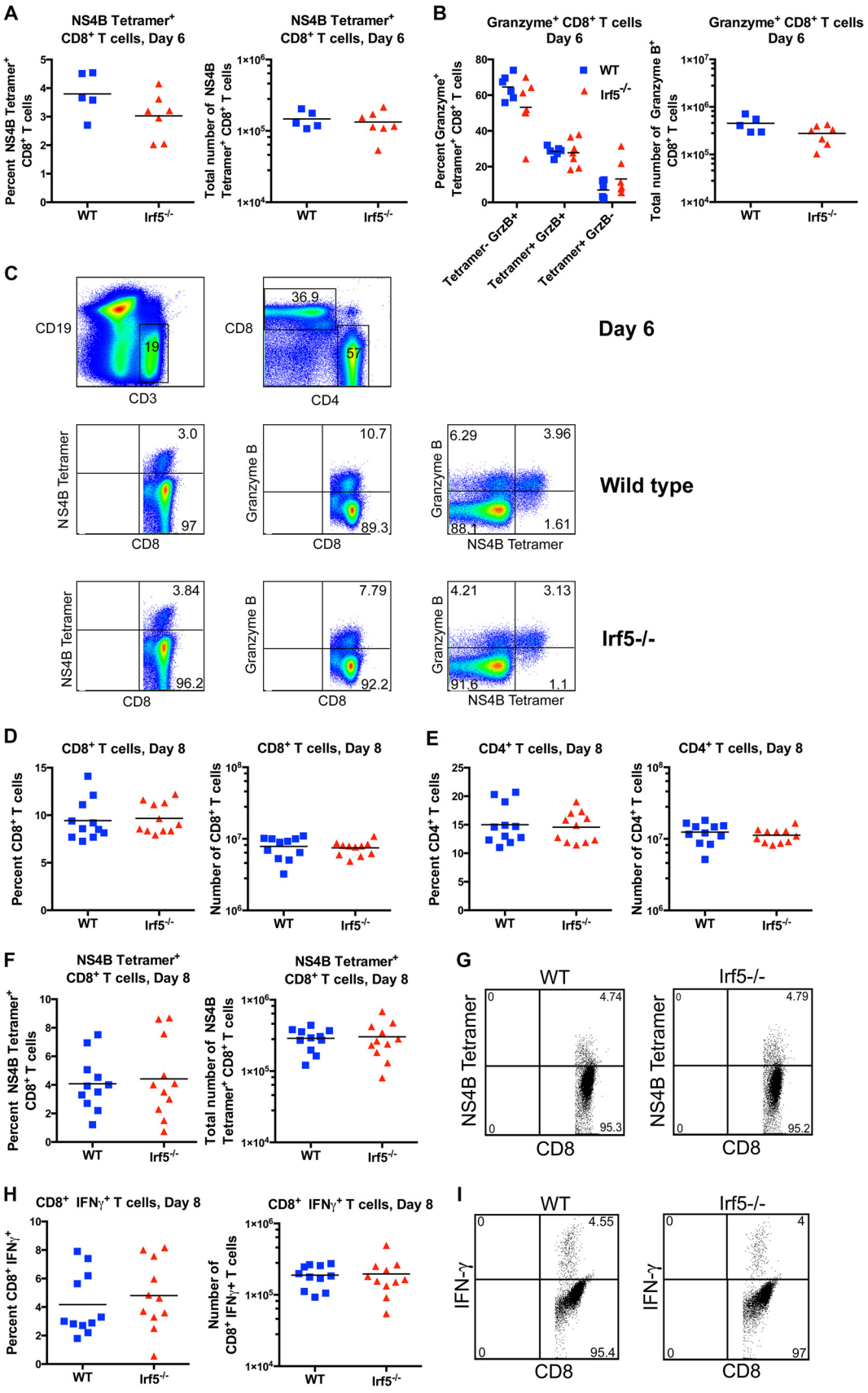

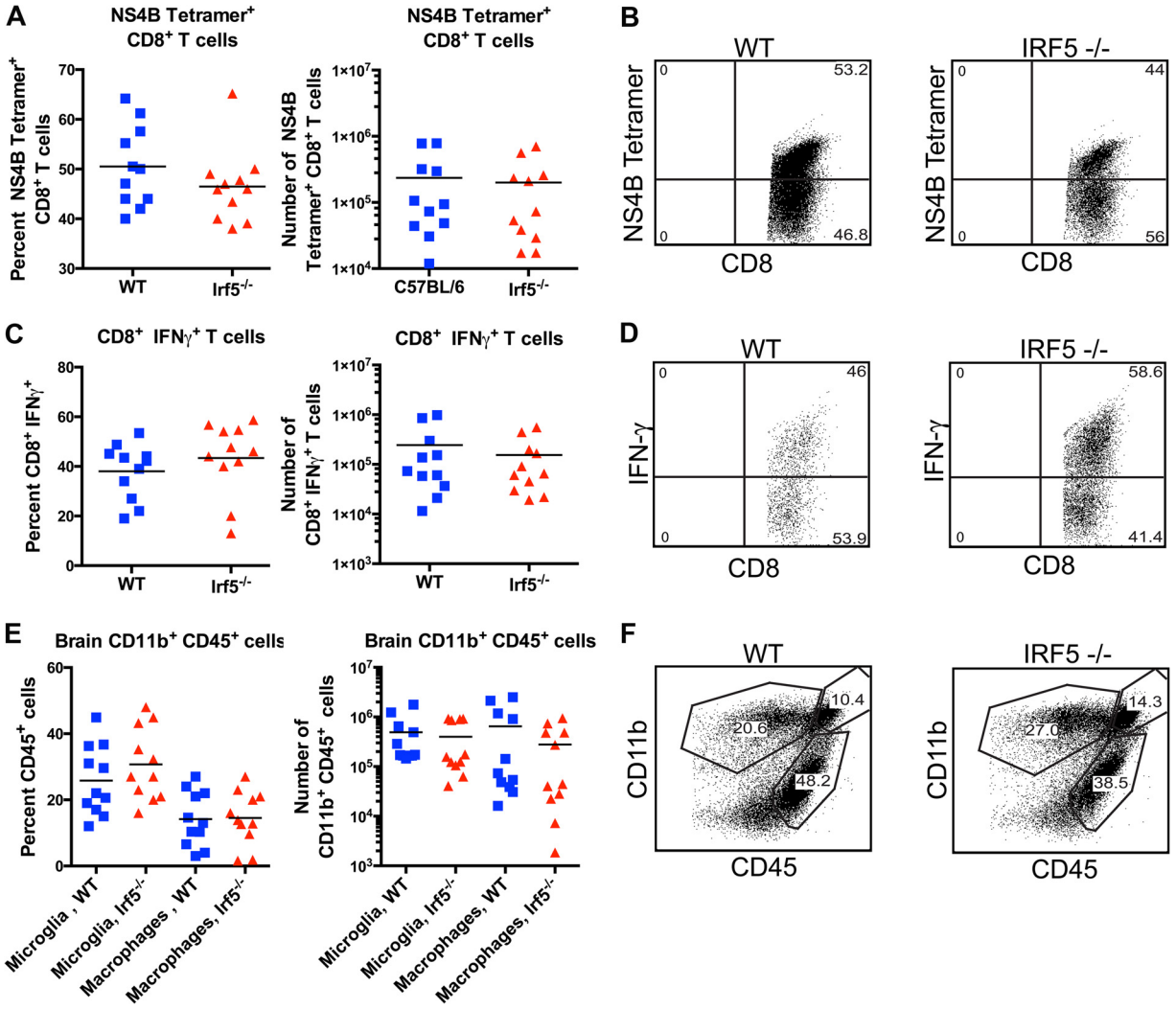

FIG 7 Immune cell responses in the brain after WNV infection. WT and *Irf5*$^{-/-}$ mice were infected with 10^2 PFU of WNV in the footpad. Brain leukocytes were harvested and analyzed by flow cytometry at 8 days after infection. Percentages and numbers of NS4B tetramer$^+$ CD8$^+$ T cells (A), IFN-γ expressing CD8$^+$ T cells after restimulation with an immunodominant NS4B peptide (C), and microglia (CD11b$^+$CD45^{lo}) and macrophages (CD11b$^+$CD45^{hi}) (E) are shown. Symbols represent individual mice. (B, D, and F) Representative flow cytometry plots of NS4B tetramer$^+$ (B), IFN-γ$^+$ CD8$^+$ T cells (D), and microglia/macrophages (F) from the brains of infected WT and *Irf5*$^{-/-}$ mice. Numbers indicate the percentage of cells in each quadrant. The results are the pooled from two independent experiments, with a total of 11 mice per group. None of the differences were statistically significant, as judged by the Mann-Whitney test.

produced less IFN-α and IFN-β in response to TLR4 and TLR9 agonists (24, 47, 48) or myxoma virus (49). Analogous cytokine induction studies with WNV have shown greater type I IFN production from conventional myeloid compared to plasmacytoid dendritic cells (50). Alternatively, some of the earlier studies may have used mice carrying the Dock2 mutation, which independently affects migration or activity of IFN-producing immune cells (26, 27).

We did observe a role for IRF5 in regulating expression of proinflammatory cytokine and chemokine responses, especially at early times after WNV infection in serum and the DLN. This result agrees with studies in *Irf5*$^{-/-}$ mice that used other inflammatory agonists or viruses as stimuli (18, 20, 21, 23). Nonetheless, the signaling pathway that induces these proinflammatory molecules remains uncertain. Although IRF5-dependent cytokine induction after TLR agonist stimulation occurs via MyD88- and/or TRIF-dependent pathways (18, 51), after viral infection it also depends on RLR- and MAVS-dependent signals (14, 52). Indeed, IRF5 has

FIG 6 T cell responses in the spleen after WNV infection. WT and *Irf5*$^{-/-}$ mice were infected with 10^2 PFU of WNV in the footpad. Splenocytes were harvested and analyzed by flow cytometry at day 6 (A to C) or 8 (D to I) after infection. The percentages and numbers of NS4B tetramer$^+$ CD8$^+$ T cells (A and F), granzyme B$^+$ CD8$^+$ T cells (B), total CD8$^+$ T cells (D), total CD4$^+$ T cells (E), or IFN-γ-expressing CD8$^+$ T cells after restimulation with an immunodominant NS4B peptide (H) are shown. Symbols represent individual mice. (C, G, and I) Representative flow cytometry plots of NS4B tetramer$^+$ (C and G), granzyme B$^+$ (C), and IFN-γ$^+$ CD8$^+$ (I) T cells from WT and *Irf5*$^{-/-}$ mice at days 6 or 8 after infection. Numbers indicate the percentage of cells in each quadrant. The results are pooled from two independent experiments with a total of 5 to 11 mice per group depending on the experiment. None of the comparisons were statistically different, as judged by the Mann-Whitney test.

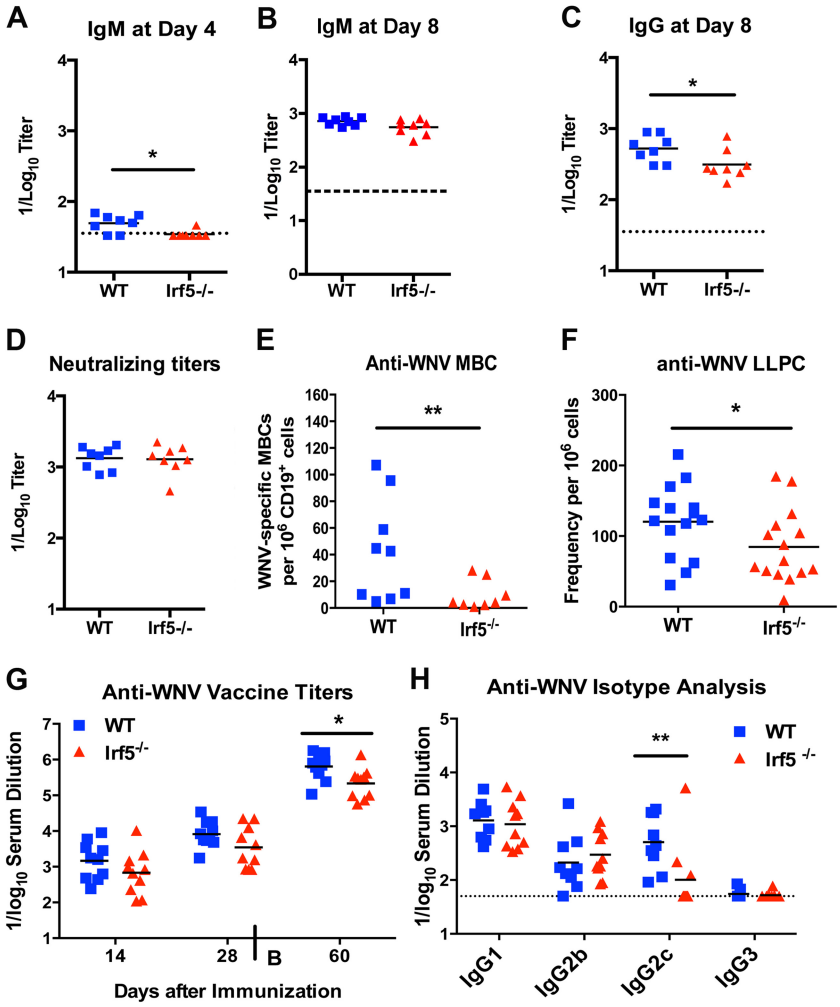

FIG 8 B cell responses to live and inactivated WNV in WT and *Irf5*$^{-/-}$ mice. (A to C) Serum was obtained from WNV-infected WT and *Irf5*$^{-/-}$ mice, and the IgM levels at days 4 (A) and 8 (B) or the IgG levels at day 8 (C) after infection were measured by ELISA for reactivity with the WNV E protein. (D) Neutralizing antibody titers were determined by a focus-reduction assay from serum at day 8. The results are shown as a scatter plot and represent samples from seven to eight mice per group. The data are plotted as the reciprocal $\log_{10}$ titer, and dotted lines indicate the limit of sensitivity of the ELISA. (E to H) B cell immune responses to inactivated WNV-Kunjin vaccine. WT and *Irf5*$^{-/-}$ mice (n = 10 to 15 from two to three independent experiments) were immunized with adjuvanted WNV-Kunjin vaccine at day 0 and boosted at day 30. After vaccination, serum was obtained (days 14, 28, and 60), and splenic MBCs and bone marrow LLPCs (day 60) were harvested. (E) WNV-specific MBCs were determined by limiting dilution assay 6 days after polyclonal stimulation, as described in Materials and Methods. (F) WNV-specific LLPCs were determined by ELISPOT analysis. (G) Total Anti-WNV E IgG titers were determined from serum at the indicated days by ELISA. (H) Isotype analysis of WNV-specific MAbs was determined by ELISA on serum 28 days after immunization. Asterisks indicate statistical significance (*, $P < 0.05$; **, $P < 0.01$), as judged by the Mann-Whitney test.

been shown to interact in a complex with RIG-I and MAVS via coimmunoprecipitation and immunoblotting experiments (14, 21, 53). Under certain circumstances, RLR signaling can antagonize IRF5-dependent cytokine production as activated IRF3 can bind dominantly, relative to IRF5, to the *Il12b* gene promoter and interfere with the TLR-induced assembly of a transcription-factor complex (54). As an additional level of regulation, histone deacetylases and acetyltransferases associate directly with IRF5 and modulate its transcriptional activity (55). Further studies in primary cells are needed to define the mechanistic intermediates that link IRF5 activation and signaling to cytokine induction after WNV infection.

Among the most significant phenotypes observed was the impact of IRF5 on leukocyte numbers in the DLN before and after WNV infection. This unexpected phenotype was not due to differences in virus trafficking or local replication because WNV titers were similar between WT and *Irf5*$^{-/-}$ mice within 2 days of infection. Rather, our data suggest that both homeostatically and downstream of virus infection and pathogen detection pathways, IRF5 regulates expression of cytokines and chemokines that shape cellular trafficking into the DLN and activation of key cell types once they enter. In the absence of IRF5, fewer T cells, B cells, NK cells, macrophages, and dendritic cells were present in the DLN at day 2 after infection, and several lymphocyte subsets expressed smaller amounts of the activation marker CD69. Given that we observed no difference in WNV replication in dendritic cells from WT and *Irf5*$^{-/-}$ mice (14) or in neurons after intracranial infection of WT and *Irf5*$^{-/-}$ mice, our data are most consistent with a cell-extrinsic indirect antiviral function of IRF5 that reflects its immunomodulatory activity. Proinflammatory and leukocyte re-

cruitment functions of IRF5 in the DLN have implications for its linkage to SLE, which can feature upregulated expression of IRF5 (56, 57), and for the metastatic potential of tumors where IRF5 expression is downregulated (58, 59).

Part of the enhanced vulnerability of *Irf5*$^{-/-}$ mice to WNV infection also may be associated with defects in B cell responses. Despite the increase in viral infection and antigen in peripheral tissues, we observed blunted IgM and IgG responses at early time points. This could impact WNV pathogenesis, since the early humoral response is critical for controlling viremia. Even small differences in WNV-specific IgM levels at early times after infection affect viral dissemination to the brain and clinical outcome (28, 32). Because of the possible confounding influence of enhanced WNV infection and antigen burden on B cell responses in *Irf5*$^{-/-}$ mice, we also performed immunization studies with a H_2O_2-inactivated nonreplicating WNV-Kunjin virus strain (30). In these experiments, we observed defects in *Irf5*$^{-/-}$ mice after boosting in the magnitude and isotype skewing of the serum IgG responses, as well as the total numbers of antigen-specific LLPCs and MBCs. These results are consistent with the concept that IRF5 has a B-cell-intrinsic function through its ability to modulate the plasma cell maturation factor, Blimp-1 (43). While our data agree with the trends identified in a prior study showing altered isotype skewing in response to T-dependent or polyomavirus infection (29), the magnitude of the phenotype after WNV infection was subtle. Indeed, in a study by Fang et al., the antibody phenotype was more pronounced in the *Irf5*$^{-/-}$ mice compared to *Irf5*$^{cre/cre}$ mice (29), which could reflect the effect of the adventitious *Dock2* mutation on T_H2-type effects (24).

In summary, our study shows that *Irf5*$^{-/-}$ mice were more vulnerable to lethal WNV infection. This phenotype was associated with defects in accumulation and activation of immune cells in the DLN that likely reflected the loss of IRF5-dependent expression of proinflammatory cytokines and chemokines, with possible subordinate effects on the type I IFN response. The altered DLN response and deficits in the early antibody response correlated with increased WNV infection in the spleen and the bloodstream, which resulted in higher peak titers in the brain and spinal cord. Future studies with conditionally targeted mice are planned to define the specific cell types that use IRF5 to shape LN responses after viral infection or immunogen exposure. Given the wide range of effects of loss-of-function and gain-of-function IRF5 alleles, an improved understanding of its specific functions in innate and adaptive immunity could facilitate strategies that ameliorate clinical outcomes in the context of viral infection, autoimmunity, and neoplastic disease.

ACKNOWLEDGMENTS

National Institutes of Health (NIH) grants U19 AI083019, U19 AI106772, R01 AI104972, and R01 AI104002 supported this study.

We thank the NIH Tetramer Core Facility at Emory University for providing NS4B-specific tetramers, P. Pitha for the *Irf5*$^{fl/fl}$ mice, M. Slifka and I. Amanna for the inactivated WNV-Kunjin vaccine, and Michelle Noll and Qing Tan for technical assistance with the mice.

REFERENCES

1. **Honda K, Taniguchi T.** 2006. IRFs: master regulators of signaling by Toll-like receptors and cytosolic pattern-recognition receptors. Nat. Rev. Immunol. **6:**644–658. http://dx.doi.org/10.1038/nri1900.
2. **Platanias LC.** 2005. Mechanisms of type-I- and type-II-interferon-mediated signaling. Nat. Rev. Immunol. **5:**375–386. http://dx.doi.org/10.1038/nri1604.
3. **Schoggins JW, Rice CM.** 2011. Interferon-stimulated genes and their antiviral effector functions. Curr. Opin. Virol. **1:**519–525. http://dx.doi.org/10.1016/j.coviro.2011.10.008.
4. **Honda K, Yanai H, Negishi H, Asagiri M, Sato M, Mizutani T, Shimada N, Ohba Y, Takaoka A, Yoshida N, Taniguchi T.** 2005. IRF-7 is the master regulator of type-I interferon-dependent immune responses. Nature **434:**772–777. http://dx.doi.org/10.1038/nature03464.
5. **Daffis S, Suthar MS, Szretter KJ, Gale M, Jr., Diamond MS.** 2009. Induction of IFN-beta and the innate antiviral response in myeloid cells occurs through an IPS-1-dependent signal that does not require IRF-3 and IRF-7. PLoS Pathog. **5:**e1000607. http://dx.doi.org/10.1371/journal.ppat.1000607.
6. **Steinberg C, Eisenacher K, Gross O, Reindl W, Schmitz F, Ruland J, Krug A.** 2009. The IFN regulatory factor 7-dependent type I IFN response is not essential for early resistance against murine cytomegalovirus infection. Eur. J. Immunol. **39:**1007–1018. http://dx.doi.org/10.1002/eji.200838814.
7. **Chen HW, King K, Tu J, Sanchez M, Luster AD, Shresta S.** 2013. The roles of IRF-3 and IRF-7 in innate antiviral immunity against dengue virus. J. Immunol. **191:**4194–4201. http://dx.doi.org/10.4049/jimmunol.1300799.
8. **Thackray LB, Duan E, Lazear HM, Kambal A, Schreiber RD, Diamond MS, Virgin HW.** 2012. Critical role for interferon regulatory factor 3 (IRF-3) and IRF-7 in type I interferon-mediated control of murine norovirus replication. J. Virol. **86:**13515–13523. http://dx.doi.org/10.1128/JVI.01824-12.
9. **Schilte C, Buckwalter MR, Laird ME, Diamond MS, Schwartz O, Albert ML.** 2012. Cutting edge: independent roles for IRF-3 and IRF-7 in hematopoietic and nonhematopoietic cells during host response to Chikungunya infection. J. Immunol. **188:**2967–2971. http://dx.doi.org/10.4049/jimmunol.1103185.
10. **Daffis S, Lazear HM, Liu WJ, Audsley M, Engle M, Khromykh AA, Diamond MS.** 2011. The naturally attenuated Kunjin strain of West Nile virus shows enhanced sensitivity to the host type I interferon response. J. Virol. **85:**5664–5668. http://dx.doi.org/10.1128/JVI.00232-11.
11. **Rudd PA, Wilson J, Gardner J, Larcher T, Babarit C, Le TT, Anraku I, Kumagai Y, Loo YM, Gale M, Jr., Akira S, Khromykh AA, Suhrbier A.** 2012. Interferon response factors 3 and 7 protect against Chikungunya virus hemorrhagic fever and shock. J. Virol. **86:**9888–9898. http://dx.doi.org/10.1128/JVI.00956-12.
12. **Suthar MS, Ma DY, Thomas S, Lund JM, Zhang N, Daffis S, Rudensky AY, Bevan MJ, Clark EA, Murali-Krishna KJ, Diamond MS, Gale M.** 2010. IPS-1 is essential for the control of West Nile virus infection and immunity. PLoS Pathog. **6:**e1000757. http://dx.doi.org/10.1371/journal.ppat.1000757.
13. **You F, Wang P, Yang L, Yang G, Zhao YO, Qian F, Walker W, Sutton R, Montgomery R, Lin R, Iwasaki A, Fikrig E.** 2013. ELF4 is critical for induction of type I interferon and the host antiviral response. Nat. Immunol. **14:**1237–1246. http://dx.doi.org/10.1038/ni.2756.
14. **Lazear HM, Lancaster A, Wilkins C, Suthar MS, Huang A, Vick SC, Clepper L, Thackray L, Brassil MM, Virgin HW, Nikolich-Zugich J, Moses AV, Gale M, Jr., Fruh K, Diamond MS.** 2013. IRF-3, IRF-5, and IRF-7 coordinately regulate the type I IFN response in myeloid dendritic cells downstream of MAVS signaling. PLoS Pathog. **9:**e1003118. http://dx.doi.org/10.1371/journal.ppat.1003118.
15. **Barnes BJ, Kellum MJ, Field AE, Pitha PM.** 2002. Multiple regulatory domains of IRF-5 control activation, cellular localization, and induction of chemokines that mediate recruitment of T lymphocytes. Mol. Cell. Biol. **22:**5721–5740. http://dx.doi.org/10.1128/MCB.22.16.5721-5740.2002.
16. **Barnes BJ, Moore PA, Pitha PM.** 2001. Virus-specific activation of a novel interferon regulatory factor, IRF-5, results in the induction of distinct interferon alpha genes. J. Biol. Chem. **276:**23382–23390. http://dx.doi.org/10.1074/jbc.M101216200.
17. **Barnes BJ, Field AE, Pitha-Rowe PM.** 2003. Virus-induced heterodimer formation between IRF-5 and IRF-7 modulates assembly of the IFNA enhanceosome in vivo and transcriptional activity of IFNA genes. J. Biol. Chem. **278:**16630–16641. http://dx.doi.org/10.1074/jbc.M212609200.
18. **Takaoka A, Yanai H, Kondo S, Duncan G, Negishi H, Mizutani T, Kano S, Honda K, Ohba Y, Mak TW, Taniguchi T.** 2005. Integral role of IRF-5 in the gene induction programme activated by Toll-like receptors. Nature **434:**243–249. http://dx.doi.org/10.1038/nature03308.
19. **Schoenemeyer A, Barnes BJ, Mancl ME, Latz E, Goutagny N, Pitha PM, Fitzgerald KA, Golenbock DT.** 2005. The interferon regulatory factor,

IRF5, is a central mediator of Toll-like receptor 7 signaling. J. Biol. Chem. **280:**17005–17012. http://dx.doi.org/10.1074/jbc.M412584200.
20. **Paun A, Reinert JT, Jiang Z, Medin C, Balkhi MY, Fitzgerald KA, Pitha PM.** 2008. Functional characterization of murine interferon regulatory factor 5 (IRF-5) and its role in the innate antiviral response. J. Biol. Chem. **283:**14295–14308. http://dx.doi.org/10.1074/jbc.M800501200.
21. **Yanai H, Chen HM, Inuzuka T, Kondo S, Mak TW, Takaoka A, Honda K, Taniguchi T.** 2007. Role of IFN regulatory factor 5 transcription factor in antiviral immunity and tumor suppression. Proc. Natl. Acad. Sci. U. S. A. **104:**3402–3407. http://dx.doi.org/10.1073/pnas.0611559104.
22. **Barnes BJ, Richards J, Mancl M, Hanash S, Beretta L, Pitha PM.** 2004. Global and distinct targets of IRF-5 and IRF-7 during innate response to viral infection. J. Biol. Chem. **279:**45194–45207. http://dx.doi.org/10.1074/jbc.M400726200.
23. **Purtha WE, Swiecki M, Colonna M, Diamond MS, Bhattacharya D.** 2012. Spontaneous mutation of the Dock2 gene in Irf5$^{-/-}$ mice complicates interpretation of type I interferon production and antibody responses. Proc. Natl. Acad. Sci. U. S. A. **109:**E898–E904. http://dx.doi.org/10.1073/pnas.1118155109.
24. **Yasuda K, Nundel K, Watkins AA, Dhawan T, Bonegio RG, Ubellacker JM, Marshak-Rothstein A, Rifkin IR.** 2013. Phenotype and function of B cells and dendritic cells from interferon regulatory factor 5-deficient mice with and without a mutation in DOCK2. Int. Immunol. **25:**295–306. http://dx.doi.org/10.1093/intimm/dxs114.
25. **Fukui Y, Hashimoto O, Sanui T, Oono T, Koga H, Abe M, Inayoshi A, Noda M, Oike M, Shirai T, Sasazuki T.** 2001. Haematopoietic cell-specific CDM family protein DOCK2 is essential for lymphocyte migration. Nature **412:**826–831. http://dx.doi.org/10.1038/35090591.
26. **Gotoh K, Tanaka Y, Nishikimi A, Inayoshi A, Enjoji M, Takayanagi R, Sasazuki T, Fukui Y.** 2008. Differential requirement for DOCK2 in migration of plasmacytoid dendritic cells versus myeloid dendritic cells. Blood **111:**2973–2976. http://dx.doi.org/10.1182/blood-2007-09-112169.
27. **Gotoh K, Tanaka Y, Nishikimi A, Nakamura R, Yamada H, Maeda N, Ishikawa T, Hoshino K, Uruno T, Cao Q, Higashi S, Kawaguchi Y, Enjoji M, Takayanagi R, Kaisho T, Yoshikai Y, Fukui Y.** 2010. Selective control of type I IFN induction by the Rac activator DOCK2 during TLR-mediated plasmacytoid dendritic cell activation. J. Exp. Med. **207:**721–730. http://dx.doi.org/10.1084/jem.20091776.
28. **Diamond MS, Shrestha B, Marri A, Mahan D, Engle M.** 2003. B cells and antibody play critical roles in the immediate defense of disseminated infection by West Nile encephalitis virus. J. Virol. **77:**2578–2586. http://dx.doi.org/10.1128/JVI.77.4.2578-2586.2003.
29. **Fang CM, Roy S, Nielsen E, Paul M, Maul R, Paun A, Koentgen F, Raval FM, Szomolanyi-Tsuda E, Pitha PM.** 2012. Unique contribution of IRF-5-Ikaros axis to the B-cell IgG2a response. Genes Immun. **13:**421–430. http://dx.doi.org/10.1038/gene.2012.10.
30. **Pinto AK, Richner JM, Poore EA, Patil PP, Amanna IJ, Slifka MK, Diamond MS.** 2013. A hydrogen peroxide-inactivated virus vaccine elicits humoral and cellular immunity and protects against lethal West Nile virus infection in aged mice. J. Virol. **87:**1926–1936. http://dx.doi.org/10.1128/JVI.02903-12.
31. **Mehlhop E, Diamond MS.** 2006. Protective immune responses against West Nile virus are primed by distinct complement activation pathways. J. Exp. Med. **203:**1371–1381. http://dx.doi.org/10.1084/jem.20052388.
32. **Diamond MS, Sitati E, Friend L, Shrestha B, Higgs S, Engle M.** 2003. A critical role for induced IgM in the protection against West Nile virus infection. J. Exp. Med. **198:**1853–1862. http://dx.doi.org/10.1084/jem.20031223.
33. **Purtha WE, Tedder TF, Johnson S, Bhattacharya D, Diamond MS.** 2011. Memory B cells but not long-lived plasma cells possess antigen specificities for viral escape mutants J. Exp. Med. **208:**2599–2606. http://dx.doi.org/10.1084/jem.20110740.
34. **Purtha WE, Myers N, Mitaksov V, Sitati E, Connolly J, Fremont DH, Hansen TH, Diamond MS.** 2007. Antigen-specific cytotoxic T lymphocytes protect against lethal West Nile virus encephalitis. Eur. J. Immunol. **37:**1845–1854. http://dx.doi.org/10.1002/eji.200737192.
35. **Jin YH, Kim SJ, So EY, Meng L, Colonna M, Kim BS.** 2012. Melanoma differentiation-associated gene 5 is critical for protection against Theiler's virus-induced demyelinating disease. J. Virol. **86:**1531–1543. http://dx.doi.org/10.1128/JVI.06457-11.
36. **Daffis S, Samuel MA, Suthar MS, Gale M, Jr., Diamond MS.** 2008. Toll-like receptor 3 has a protective role against West Nile virus infection. J. Virol. **82:**10349–10358. http://dx.doi.org/10.1128/JVI.00935-08.
37. **Szretter KJ, Daffis S, Patel J, Suthar MS, Klein RS, Gale M, Jr., Diamond MS.** 2010. The innate immune adaptor molecule MyD88 restricts West Nile replication and spread in neurons of the central nervous system. J. Virol. **84:**12125–12138. http://dx.doi.org/10.1128/JVI.01026-10.
38. **Purtha WE, Chachu KA, Virgin HW, Diamond MS.** 2008. Early B-cell activation after West Nile virus infection requires alpha/beta interferon but not antigen receptor signaling. J. Virol. **82:**10964–10974. http://dx.doi.org/10.1128/JVI.01646-08.
39. **Sitati E, Diamond MS.** 2006. CD4+ T Cell responses are required for clearance of West Nile Virus from the central nervous system. J. Virol. **80:**12060–12069. http://dx.doi.org/10.1128/JVI.01650-06.
40. **Shrestha B, Diamond MS.** 2004. The role of CD8+ T cells in the control of West Nile virus infection. J. Virol. **78:**8312–8321. http://dx.doi.org/10.1128/JVI.78.15.8312-8321.2004.
41. **Brien JD, Uhrlaub JL, Hirsch A, Wiley CA, Nikolich-Zugich J.** 2009. Key role of T cell defects in age-related vulnerability to West Nile virus. J. Exp. Med. **206:**2735–2745. http://dx.doi.org/10.1084/jem.20090222.
42. **Brien JD, Uhrlaub JL, Nikolich-Zugich J.** 2007. Protective capacity and epitope specificity of CD8$^+$ T cells responding to lethal West Nile virus infection. Eur. J. Immunol. **37:**1855–1863. http://dx.doi.org/10.1002/eji.200737196.
43. **Lien C, Fang CM, Huso D, Livak F, Lu R, Pitha PM.** 2010. Critical role of IRF-5 in regulation of B-cell differentiation. Proc. Natl. Acad. Sci. U. S. A. **107:**4664–4668. http://dx.doi.org/10.1073/pnas.0911193107.
44. **Savitsky DA, Yanai H, Tamura T, Taniguchi T, Honda K.** 2010. Contribution of IRF5 in B cells to the development of murine SLE-like disease through its transcriptional control of the IgG2a locus. Proc. Natl. Acad. Sci. U. S. A. **107:**10154–10159. http://dx.doi.org/10.1073/pnas.1005599107.
45. **Chambers TJ, Droll DA, Walton AH, Schwartz J, Wold WS, Nickells J.** 2008. West Nile 25A virus infection of B-cell-deficient ((micro)MT) mice: characterization of neuroinvasiveness and pseudoreversion of the viral envelope protein. J. Gen. Virol. **89:**627–635. http://dx.doi.org/10.1099/vir.0.83297-0.
46. **Shrestha B, Wang T, Samuel MA, Whitby K, Craft J, Fikrig E, Diamond MS.** 2006. Gamma interferon plays a crucial early antiviral role in protection against West Nile virus infection. J. Virol. **80:**5338–5348. http://dx.doi.org/10.1128/JVI.00274-06.
47. **Yasuda K, Richez C, Maciaszek JW, Agrawal N, Akira S, Marshak-Rothstein A, Rifkin IR.** 2007. Murine dendritic cell type I IFN production induced by human IgG-RNA immune complexes is IFN regulatory factor (IRF)5 and IRF7 dependent and is required for IL-6 production. J. Immunol. **178:**6876–6885. http://dx.doi.org/10.4049/jimmunol.178.11.6876.
48. **Richez C, Yasuda K, Watkins AA, Akira S, Lafyatis R, van Seventer JM, Rifkin IR.** 2009. TLR4 ligands induce IFN-alpha production by mouse conventional dendritic cells and human monocytes after IFN-beta priming. J. Immunol. **182:**820–828. http://dx.doi.org/10.4049/jimmunol.182.2.820.
49. **Dai P, Cao H, Merghoub T, Avogadri F, Wang W, Parikh T, Fang CM, Pitha PM, Fitzgerald KA, Rahman MM, McFadden G, Hu X, Houghton AN, Shuman S, Deng L.** 2011. Myxoma virus induces type I interferon production in murine plasmacytoid dendritic cells via a TLR9/MyD88-, IRF5/IRF7-, and IFNAR-dependent pathway. J. Virol. **85:**10814–10825. http://dx.doi.org/10.1128/JVI.00104-11.
50. **Gitlin L, Barchet W, Gilfillan S, Cella M, Beutler B, Flavell RA, Diamond MS, Colonna M.** 2006. Essential role of *mda-5* in type I IFN responses to polyriboinosinic:polyribocytidylic acid and encephalomyocarditis picornavirus. Proc. Natl. Acad. Sci. U. S. A. **103:**8459–8464. http://dx.doi.org/10.1073/pnas.0603082103.
51. **Ouyang X, Negishi H, Takeda R, Fujita Y, Taniguchi T, Honda K.** 2007. Cooperation between MyD88 and TRIF pathways in TLR synergy via IRF5 activation. Biochem. Biophys. Res. Commun. **354:**1045–1051. http://dx.doi.org/10.1016/j.bbrc.2007.01.090.
52. **Nandakumar R, Finsterbusch K, Lipps C, Neumann B, Grashoff M, Nair S, Hochnadel I, Lienenklaus S, Wappler I, Steinmann E, Hauser H, Pietschmann T, Kroger A.** 2013. Hepatitis C virus replication in mouse cells is restricted by IFN-dependent and -independent mechanisms. Gastroenterology **145:**1414–1423 e1411. http://dx.doi.org/10.1053/j.gastro.2013.08.037.
53. **Li S, Wang L, Berman M, Kong YY, Dorf ME.** 2011. Mapping a dynamic innate immunity protein interaction network regulating type I interferon production. Immunity **35:**426–440. http://dx.doi.org/10.1016/j.immuni.2011.06.014.
54. **Negishi H, Yanai H, Nakajima A, Koshiba R, Atarashi K, Matsuda A, Matsuki K, Miki S, Doi T, Aderem A, Nishio J, Smale ST, Honda K,**

Taniguchi T. 2012. Cross-interference of RLR and TLR signaling pathways modulates antibacterial T cell responses. Nat. Immunol. **13:**659-666. http://dx.doi.org/10.1038/ni.2307.

55. **Feng D, Sangster-Guity N, Stone R, Korczeniewska J, Mancl ME, Fitzgerald-Bocarsly P, Barnes BJ.** 2010. Differential requirement of histone acetylase and deacetylase activities for IRF5-mediated proinflammatory cytokine expression. J. Immunol. **185:**6003–6012. http://dx.doi.org/10.4049/jimmunol.1000482.
56. **Sigurdsson S, Nordmark G, Goring HH, Lindroos K, Wiman AC, Sturfelt G, Jonsen A, Rantapaa-Dahlqvist S, Moller B, Kere J, Koskenmies S, Widen E, Eloranta ML, Julkunen H, Kristjansdottir H, Steinsson K, Alm G, Ronnblom L, Syvanen AC.** 2005. Polymorphisms in the tyrosine kinase 2 and interferon regulatory factor 5 genes are associated with systemic lupus erythematosus. Am. J. Hum. Genet. **76:**528–537. http://dx.doi.org/10.1086/428480.
57. **Feng D, Stone RC, Eloranta ML, Sangster-Guity N, Nordmark G, Sigurdsson S, Wang C, Alm G, Syvanen AC, Ronnblom L, Barnes BJ.** 2010. Genetic variants and disease-associated factors contribute to enhanced interferon regulatory factor 5 expression in blood cells of patients with systemic lupus erythematosus. Arthritis Rheum. **62:**562–573.
58. **Bi X, Hameed M, Mirani N, Pimenta EM, Anari J, Barnes BJ.** 2011. Loss of interferon regulatory factor 5 (IRF5) expression in human ductal carcinoma correlates with disease stage and contributes to metastasis. Breast Cancer Res. **13:**R111. http://dx.doi.org/10.1186/bcr3053.
59. **Yamashita M, Toyota M, Suzuki H, Nojima M, Yamamoto E, Kamimae S, Watanabe Y, Kai M, Akashi H, Maruyama R, Sasaki Y, Yamano H, Sugai T, Shinomura Y, Imai K, Tokino T, Itoh F.** 2010. DNA methylation of interferon regulatory factors in gastric cancer and noncancerous gastric mucosae. Cancer Sci. **101:**1708–1716. http://dx.doi.org/10.1111/j.1349-7006.2010.01581.x.